

# Communication link design at 437.5 MHz for a nanosatellite



Jorge Cantero Gómez  
Department of Radio Science and Engineering  
School of Electrical Engineering  
Aalto University

A final project submitted for the degree of  
*Telecommunications Engineering*

Supervised by D.Sc. (Tech.) Jaan Praks  
June 2013

|   |                   |                        |
|---|-------------------|------------------------|
| Author: Jorge Cantero Gómez   |                   |                        |
| Title: Communication link design at 437.5 MHz for a nanosatellite   |                   |                        |
| Date: June 2013   | Language: English | Number of pages: 10+61 |
| Department of Radio Science and Engineering   |                   |                        |
| Professorship: Space Technology   |                   | Code: S-92             |
| Supervisor and instructor: D.Sc. (Tech.) Jaan Praks   |                   |                        |
| <p>The goal of this work was to design communication solution for the nanosatellite Aalto-2 which is an educational oriented CubeSat project started in 2012 by Aalto University, Finland. The main objective of the Aalto-2 project is to build a nanosatellite for ionospheric studies in the framework of QB50 project. This mission has the goal of studying the lower thermosphere making use of 50 small satellites.</p> <p>Every small satellite in the QB50 satellite constellation should be equipped with a radio communication link and should be able to send the collected scientific measurements, telemetry and health status to the ground as well as receive commands from Earth.</p> <p>Main focus of this study was design the communication link and the antennas according to the requirements set by QB50 consortium. Three communication studies have been done: design and optimization of antennas with the aim of having a good radiation pattern; data budget, in order to know the volume of data that can be downloaded every day; and link budget, to assure a good communication with the ground station. For this purpose, three powerful simulation tools such as STK, CST Studio and AMSAT-IARU Link Model have been used.</p> <p>As a result of this work, a complete communication scheme for the Aalto-2 satellite was designed. The design is in accordance with QB50 requirements and includes a design of an omnidirectional antenna and data budget suitable for QB50 scientific measurements.</p> |                   |                        |
| Keywords: Aalto-2, CubeSat, QB50, Antenna, Data budget, Link budget   |                   |                        |

## Preface

This final project has been carried out in the Department of Radio Science and Engineering of Aalto University between February 2013 and June 2013 under the supervision of D.Sc. (Tech.) Jaan Praks. It has been very pleasant to gain knowledge in an area that I love, the space technology. Working in a laboratory helping to design and build a satellite that will be flying next year is such a dream.

First of all, I would like to thank Jaan Praks for giving me the chance of working in this project and for its attentive supervision during these months.

Secondly, I would like to thank the polytechnic University of Catalonia for making possible my stay in Finland as part of the Erasmus program as well as the staff of Aalto University for their kindness and help during my stay.

Lastly, I would like to thank especially my parents María del Carmen and Luis Javier for their support and trust during all my study years. Without them, I would not be writing these lines that conclude my telecommunications engineering studies.

Helsinki, June 2013

Jorge Cantero Gómez

# Contents

|  |      |
|--|------|
| <b>Abstract</b>  | ii   |
| <b>Preface</b>   | iii  |
| <b>Contents</b>  | iv   |
| <b>List of Tables</b>                                      | vi   |
| <b>List of Figures</b>                                     | vii  |
| <b>Symbols and acronyms</b>                                | viii |
| <b>1 Introduction</b>                                      | 1    |
| <b>2 Theoretical background of satellite communication</b> | 4    |
| 2.1 Satellites . . . . .                                   | 4    |
| 2.1.1 CubeSat standard . . . . .                           | 5    |
| 2.1.2 Satellite orbits . . . . .                           | 6    |
| 2.1.3 Two-Line Elements . . . . .                          | 11   |
| 2.2 Aalto-2 satellite . . . . .                            | 12   |
| 2.2.1 QB50 project . . . . .                               | 12   |
| 2.2.2 QB50 requirements . . . . .                          | 13   |
| 2.3 Satellite Communication . . . . .                      | 14   |
| 2.3.1 Electromagnetic radiation . . . . .                  | 14   |
| 2.3.2 Electromagnetic waves . . . . .                      | 16   |
| 2.3.3 Channel characteristics . . . . .                    | 17   |
| 2.3.4 Protocols . . . . .                                  | 19   |
| 2.4 Antennas . . . . .                                     | 21   |
| 2.4.1 Impedance . . . . .                                  | 21   |
| 2.4.2 Radiation pattern . . . . .                          | 21   |
| 2.4.3 Directivity and gain . . . . .                       | 22   |
| 2.4.4 Polarization . . . . .                               | 23   |
| 2.4.5 Bandwidth . . . . .                                  | 23   |
| 2.4.6 Antenna matching . . . . .                           | 23   |
| 2.4.7 Effective area . . . . .                             | 24   |
| 2.5 Communication budgets . . . . .                        | 25   |
| 2.5.1 Link budget . . . . .                                | 26   |
| 2.5.2 Data budget . . . . .                                | 27   |
| <b>3 Simulation tools</b>                                  | 29   |
| 3.1 Satellite Tool Kit . . . . .                           | 29   |
| 3.2 CST Studio . . . . .                                   | 29   |
| 3.3 AMSAT-IARU Link Model . . . . .                        | 30   |

|  |           |
|--|-----------|
| <b>4 Aalto-2 communication link and antenna design</b>             | <b>31</b> |
| 4.1 Communication budgets calculation . . . . .                    | 31        |
| 4.1.1 Protocol stack and frame configuration . . . . .             | 31        |
| 4.1.2 Aalto-2 orbit and link time simulations . . . . .            | 34        |
| 4.1.3 Data budget calculation . . . . .                            | 36        |
| 4.1.4 Link budget calculation . . . . .                            | 37        |
| 4.2 Aalto-2 antenna subsystem design . . . . .                     | 42        |
| 4.2.1 3D-representation of the satellite . . . . .                 | 42        |
| 4.2.2 Antenna design . . . . .                                     | 43        |
| 4.2.3 Antenna parameters . . . . .                                 | 46        |
| 4.2.4 Antenna Deployment System design . . . . .                   | 49        |
| <b>5 Future work</b>   | <b>52</b> |
| 5.1 Prototyping . . . . .  | 52        |
| 5.2 ADS testing and Radiation pattern measurements . . . . .       | 52        |
| <b>6 Conclusions</b>   | <b>53</b> |
| <b>References</b>  | <b>54</b> |
| <b>A Link budget</b>   | <b>58</b> |
| <b>B Technical drawing of the antenna holder and the end plate</b> | <b>59</b> |
| <b>C Radiation pattern</b>   | <b>60</b> |

## List of Tables

|    |   |    |
|----|---|----|
| 1  | Classification of spacecrafts by mass and cost [4]. . . . .   | 4  |
| 2  | Radio waves sorted in bands [28]. . . . .   | 15 |
| 3  | Loss due to atmospheric gases [25]. . . . .   | 19 |
| 4  | OSI model [32]. . . . .   | 19 |
| 5  | TCP header. . . . .   | 20 |
| 6  | Linear, elliptical and circular polarization [36]. . . . .  | 23 |
| 7  | Throughput at transport layer per protocol . . . . .  | 34 |
| 8  | Available connection time per day in high orbits as a function of minimal contact elevation (El). . . . . | 35 |
| 9  | Available connection time per day at lower orbits. . . . .  | 36 |
| 10 | Data budget at the beginning of the mission. . . . .  | 36 |
| 11 | Data budget at three different orbital heights. . . . .   | 37 |
| 12 | Main terms in uplink budget. . . . .  | 38 |
| 13 | Main terms in downlink budget. . . . .  | 40 |

## List of Figures

|    |  |    |
|----|--|----|
| 1  | Sputnik-1, the first object launched into orbit by man [3]. . . . .                        | 1  |
| 2  | CubeSat sizes [14]. . . . .  | 5  |
| 3  | Poly Picosatellite Orbital Deployer (P-POD) [14]. . . . .                                  | 6  |
| 4  | Characterization of an orbit and the satellite position by orbital elements [18]. . . . .  | 8  |
| 5  | Orbits depending on eccentricity [19]. . . . .   | 9  |
| 6  | Geocentric orbits [20]. . . . .  | 10 |
| 7  | '2U' CubeSat extended volume dimensions in millimeters [24]. . . . .                       | 13 |
| 8  | Electromagnetic spectrum [27]. . . . .   | 15 |
| 9  | Electromagnetic wave [30]. . . . .   | 16 |
| 10 | Isotropic, omnidirectional and directive radiation patterns [35]. . . . .                  | 22 |
| 11 | Modified TCP Header. . . . .   | 32 |
| 12 | Frame structure per layer, with three options in the transport layer. . . . .              | 33 |
| 13 | The communication frame sorted by field. . . . .   | 33 |
| 14 | The Aalto-2 satellite and the ground station simulated with STK. . . . .                   | 34 |
| 15 | Available area for communications. . . . .   | 35 |
| 16 | Aalto-2 UL budget calculated with AMSAT-IARU Link Model. . . . .                           | 39 |
| 17 | Aalto-2 DL budget calculated with AMSAT-IARU Link Model. . . . .                           | 41 |
| 18 | Mechanical drawing of the solar panel. Dimensions in millimeters [40]. . . . .             | 42 |
| 19 | 3D-representation of the Aalto-2 satellite. . . . .  | 43 |
| 20 | KySat-1 with the antennas folded over the solar panels [41]. . . . .                       | 44 |
| 21 | Two possible connections for the arms of the dipoles. . . . .                              | 45 |
| 22 | Radiation pattern for the 2 connect configurations. . . . .                                | 45 |
| 23 | Final connection for the Aalto-2 antennas. . . . .   | 46 |
| 24 | 2D radiation pattern for $\theta = 10^\circ, 45^\circ, 90^\circ$ and $135^\circ$ . . . . . | 47 |
| 25 | 2D radiation pattern for $\theta = 170^\circ$ and $S11$ graph. . . . .                     | 48 |
| 26 | Antenna holder. . . . .  | 49 |
| 27 | Texas Instruments' circuit timer CD4060BM. . . . .   | 49 |
| 28 | CD4060BM Schematic diagram showing the logical structure of the component [43]. . . . .    | 50 |
| 29 | CD4060BM Connection diagram showing the pin assignments [43]. . . . .                      | 50 |
| 30 | CD4060BM RC Oscillator diagram [43]. . . . .   | 51 |
| 31 | Antenna assembly [42]. . . . .   | 52 |
| 32 | Radiation pattern measurement in an anechoic chamber [44]. . . . .                         | 52 |

# Symbols and acronyms

## Symbols

|           |  |
|-----------|--|
| $A_R$     | Effective area of an antenna [ $m^2$ ]                                 |
| $b$       | Bit, minimum unit of information                                       |
| $\vec{B}$ | Magnetic field [ $T$ ]   |
| $B$       | Bandwidth [ $Hz$ ]   |
| $c$       | Speed of light $\approx 3 \cdot 10^8$ [ $m/s$ ]                        |
| $C$       | Capacitance [ $F$ ]  |
| $C_a$     | Mismatch coefficient   |
| $D$       | Antenna directivity  |
| $dB$      | Decibel  |
| $dB_i$    | Decibel referenced to an isotropic antenna                             |
| $\vec{E}$ | Electric field [ $N/C$ ]   |
| $e$       | Eccentricity   |
| $E_b$     | Energy per bit [ $J/b$ ]   |
| $El$      | Elevation [ $deg$ ]  |
| $f$       | Frequency [ $Hz$ ]   |
| $fr$      | Frame  |
| $G$       | Antenna gain [ $dB$ ]  |
| $Hz$      | Hertz  |
| $I$       | Electric current [ $A$ ]   |
| $\vec{k}$ | Vector wavenumber  |
| $k$       | Boltzmann's constant $\approx 1.38 \cdot 10^{-23}$ [ $J/K$ ]           |
| $L$       | Attenuation [ $dB$ ]   |
| $N_0$     | Noise power spectral density [ $W/Hz$ ]                                |
| $P$       | Power [ $dB$ ]   |
| $r$       | Distance between satellite and GS [ $m$ ]                              |
| $R$       | Resistance [ $\Omega$ ]  |
| $R_b$     | Bit rate [ $b/s$ ]   |
| $S$       | Signal power at the receiver [ $W$ ]                                   |
| $T$       | Period [ $s$ ]   |
| $T_{sys}$ | System temperature [ $K$ ]   |
| $v$       | Relative speed of the satellite [ $m/s$ ]                              |
| $X$       | Reactance [ $\Omega$ ]   |
| $Z$       | Impedance [ $\Omega$ ] ( $Z_A$ for the antenna and $Z_L$ for the load) |
| $\lambda$ | Wavelength [ $m$ ]   |
| $\mu_l$   | Antenna efficiency   |
| $\omega$  | Angular frequency [ $rad$ ]  |

## Acronyms

|                |  |
|----------------|--|
| <b>Aalto-1</b> | First nano-satellite of Aalto University (Espoo, Finland)  |
| <b>Aalto-2</b> | Second nano-satellite of Aalto University (Espoo, Finland) |
| <b>AaSI</b>    | Aalto-1 Spectral Imager                                    |
| <b>ADCS</b>    | Attitude Determination and Control System                  |
| <b>ADS</b>     | Antenna Deployment System                                  |
| <b>AGI</b>     | Analytical Graphics, Inc.                                  |
| <b>AMSAT</b>   | Radio Amateur Satellite Corporation                        |
| <b>AWGN</b>    | Additive White Gaussian Noise                              |
| <b>AX.25</b>   | Data link layer protocol                                   |
| <b>BER</b>     | Bit Error Rate   |
| <b>BW</b>      | Bandwidth  |
| <b>CCD</b>     | Carge-Couple Device  |
| <b>CDR</b>     | Critical Design Review                                     |
| <b>COM</b>     | Communications subsystem                                   |
| <b>CST</b>     | Computer Simulation Technology                             |
| <b>CubeSat</b> | Standard for nanosatellites                                |
| <b>DL</b>      | Downlink   |
| <b>EIRP</b>    | Equivalent Isotropic Radiated Power                        |
| <b>EMR</b>     | Electro-Magnetic Radiation                                 |
| <b>EPB</b>     | Electrostatic Plasma Brake, payload of Aalto-1             |
| <b>EPS</b>     | Electrical Power Supply                                    |
| <b>ESTELLE</b> | Second satellite of University of Tartu (Estonia)          |
| <b>GEO</b>     | Geostationary Orbit  |
| <b>GS</b>      | Ground Station   |
| <b>IARU</b>    | International Amateur Radio Union                          |
| <b>IEEE</b>    | Institute of Electrical and Electronics Engineers          |
| <b>ISL</b>     | Inter Satellite Link                                       |
| <b>ISO</b>     | International Organization for Standardization             |
| <b>ISS</b>     | International Space Station                                |
| <b>ITU</b>     | International Telecommunication Union                      |
| <b>LEO</b>     | Low Earth Orbit  |
| <b>LV</b>      | Launch Vehicle   |
| <b>MEO</b>     | Medium Earth Orbit   |
| <b>NASA</b>    | National Aeronautics and Space Administration              |
| <b>NLPS</b>    | Side lobe level  |
| <b>NORAD</b>   | North American Aerospace Defense Command                   |
| <b>OBC</b>     | On-Board Computer  |
| <b>OSI</b>     | Open Systems Interconnection                               |
| <b>PDR</b>     | Preliminary Design Review                                  |
| <b>PEC</b>     | Perfect Electric Conductor                                 |
| <b>PDU</b>     | Protocol Data Unit   |
| <b>PFD</b>     | Power Flux Density   |
| <b>P-POD</b>   | Poly Picosatellite Orbital Deployer                        |

|                 |   |
|-----------------|---|
| <b>QB50</b>     | International CubeSat constellation project |
| <b>RADMON</b>   | Radiation Monitor, payload of Aalto-1       |
| <b>RF</b>       | Radio Frequency                             |
| <b>RUDP</b>     | Reliable User Datagram Protocol             |
| <b>SNR</b>      | Signal to Noise Ratio                       |
| <b>SOIC</b>     | Small Outline Integrated Circuit            |
| <b>STK</b>      | Satellite Tool Kit simulation software      |
| <b>TCP</b>      | Transport Control Protocol                  |
| <b>TLE</b>      | Two-Line Elements, orbital parameters       |
| <b>TT&amp;C</b> | Tracking, Telemetry and Command             |
| <b>UDP</b>      | User Datagram Protocol                      |
| <b>UHF</b>      | Ultra High Frequency                        |
| <b>UL</b>       | Uplink                                      |
| <b>VEGA</b>     | Small orbital launch vehicle                |
| <b>VHF</b>      | Very High Frequency                         |
| <b>VLSI</b>     | Very Large Scale Integration                |

# 1 Introduction

A satellite is an object, either natural or man-made, that orbits around another body due to the gravity force. The idea of an artificial satellite appeared in May 1946 and the potential of an object visible in the sky was soon realized and scientists began soon to plan how to exploit the possibilities. Only one year later, in 1947, Arthur C. Clarke theorized that if a satellite were sent to a higher orbit, it would encounter a geosynchronous orbit, meaning that the satellite would rotate around the earth at exactly the same rate at which the earth rotates on its axis; the orbiting device would appear to hang stationary over a given point on earth. Clarke's hypotheses were supported and thus began the development of the communications sector for the space industry. [1]

Ten years later, on October 4, 1957, the first man-made satellite shown in Figure 1, Sputnik 1, was launched by the Soviet Union and only 5 years later was the first operational communications satellite giving support for public telephony and television [1]. Since then, hundreds of satellites have been launched, for both communications and scientific purposes. It is important to mention also the first satellite developed by the amateur-radio community OSCAR-1 (a simple radio transmitter in a box), which was launched on December 12, 1961, at the United States [2]. It was orbiting the Earth only for 22 days but it was a big success for the amateur radio community [2]. The first amateur satellites contained telemetry beacons which worked in frequency bands assigned to the amateur radio service by the International Telecommunication Union (ITU).

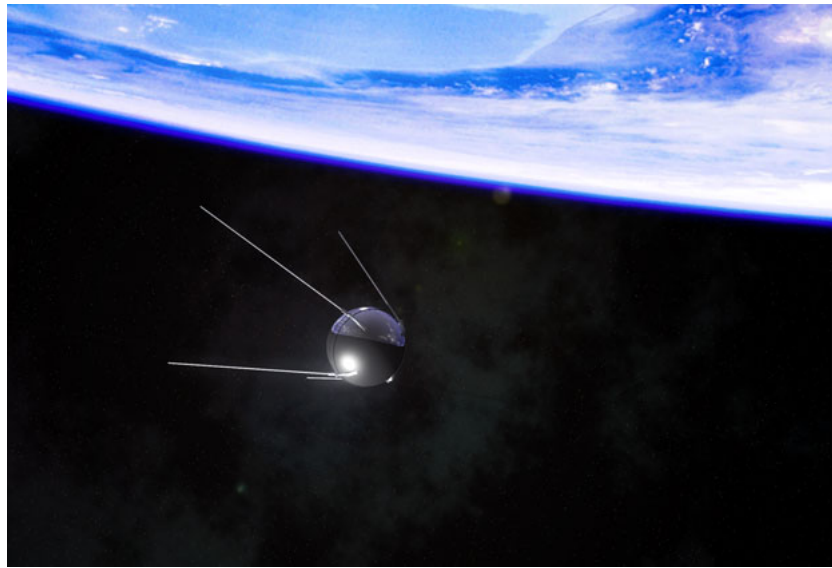


Figure 1: Sputnik-1, the first object launched into orbit by man [3].

In the 1970s, advances in Very Large Scale Integration (VLSI) electronics helped to reduce the volume of sophisticated electrical systems, as well as its mass and required power for operation. This led the emergence of modern satellite, with a smaller sizes which in turn, led to a considerable cost reduction in satellite programmes. [4]

It was at the last years of the 1970s when amateur radio enthusiasts from the University of Surrey developed a small satellite for the UK, UoSAT-1. It was launched by National Aeronautics and Space Administration (NASA) in October 1981, carrying several beacons, working at different frequencies, and a Charge-Couple Device (CCD) earth-imaging camera with 2 km resolution. The anticipated two-year lifetime was exceeded by six years, having received last signals on October 1989, before re-entering to the atmosphere. [5][6]

In the 1980s started a new era of a small sophisticated satellites, all of them using microprocessors and other VLSI technologies. A second spacecraft, the UoSAT-2, was designed and built in only 6 months for its launch in March 1984. This small satellite was still operational in 2002 after more than 18 years in orbit [7].

These two spacecraft established the modern concept of a microsatellite, an small and relatively inexpensive one, typically between 1/10th and 1/100th the mass and cost of conventional satellites [4]. It was in 1999 when another very successful small satellite standard appeared, called CubeSat. Since then, a lot of universities around the world have been used it to develop inexpensive space technology. Just as an example of the wide variety of missions carried out with CubeSat standard, it can be mentioned the in-orbit deployment of seven 1 kg CubeSats in the VEGA rocket maiden flight launched last year. These missions involved more than 250 university students from six different countries over the last four years [8]. These student satellite missions were:

- Xatcobeo (a collaboration of the University of Vigo and INTA, Spain): a mission to demonstrate software-defined radio and solar panel deployment.
- Robusta (University of Montpellier, France): a mission to test and evaluate radiation effects (low dose rate) on bipolar transistor electronic components.
- e-st@r (Politecnico di Torino, Italy): demonstration of an active 3-axis attitude determination and control system including an inertial measurement unit
- Goliat (University of Bucharest, Romania): imaging of Earth using a digital camera and in-situ measurement of radiation dose and micrometeoroid flux.
- PW-Sat (Warsaw University of Technology, Poland): a mission to test a deployable atmospheric drag augmentation device for de-orbiting CubeSats.
- MaSat-1 (Budapest University of Technology and Economics): a mission to demonstrate various spacecraft avionics, including a power conditioning system, transceiver and on-board data handling.

- UniCubeSat GG (University of Rome La Sapienza, Italy): a mission to study the gravity gradient.

The first CubeSat project in Finland, Aalto-1, was started in 2010 [9], followed quickly by Aalto-2 satellite project. Aalto-2, is also a small satellite with size about 10x10x20 and a mass under 3 kg being developed in Aalto University to be part of the QB50 project whose goal is the study of the lower thermosphere (90-320 km) using 50 small satellites [10]. Aalto-2 has passed the Preliminary Design Review (PDR) last March and nowadays Aalto-2 team is working to have engineering models of each part of the satellite ready for the Critical Design Review (CDR) next November.

This work was motivated by the need of developing the antenna deployment mechanism for the Aalto-2 satellite but, together with it, several aspects related with the communication that involve a mission like this have been studied. To assure that is possible the exchange of information between satellite and team, the link budget has been studied with AMSAT-IARU Link Model. Data budget is also needed, to know the quantity of data possible to send in the communication. This is important because Aalto-2 is considered an amateur satellite and operates within the amateur radio band, where the communication is performed at lower frequencies and at relatively slow data rate. Available connection time is calculated simulating the orbit with the software Satellite Took Kit. And finally, satellite's antennas have been designed with the software CST Studio in order to achieve a good radiation pattern to help the communications.

The antenna deployment mechanism, even being the motivation of the project, will be very similar to the one developed by the Aalto-1 team for the Aalto-1 satellite. That is why the location of this mechanism inside the Aalto-2 is genuine, but the electronics are the same that have been used in the Aalto-1 mission in order to take benefit of the knowledge already acquired.

This final project starts with a theoretical part in Chapter 2. There is explained the theory necessary to understand the issues related with telecommunications. It explains what is a satellite and how it orbits around a planet, also the satellite Aalto-2 is presented as well as the project which is part of. The next sections introduces satellite communications and its components such as the electromagnetic waves, the channel and the protocols. Finally it is presented how an antenna is characterized and communication budgets are calculated. In Chapter 3, three simulation tools used in this project are briefly explained. Chapter 4 presents the main results of the work, starting with communication budgets and finishing with the design of the Aalto-2 antennas. Finally, conclusions are presented in Chapter 6.

## 2 Theoretical background of satellite communication

### 2.1 Satellites

A satellite is an object, either natural or man-made, that orbits around another body due to the gravitational force. Since the first satellites appeared, hundreds of them have been developed and launched into space with a specific purpose such as specialised communications, earth observations, small-scale space science, technology demonstration/verification, educational and training or exploration. Depending on the purpose, satellites have different payloads to complete the mission. Typically satellites have several subsystems which are responsible of ensuring the functionality. Typical subsystems include [11][12]:

- **Communications (COM).** The communications subsystem uses transmitters and receivers, as well as antennas for sending and receiving data.
- **Tracking, Telemetry and Command (TT&C).** This subsystem monitors the on-board equipment operations and transmits this data to the earth base station. At the same time receives commands to perform equipment operation adjustments.
- **On-Board Computer (OBC).** The computer is responsible for controlling the other subsystems to keep the satellite correctly working.
- **Attitude Determination and Control System (ADCS).** This subsystem stabilizes the satellite in a correct direction if the aiming is necessary, for example, to obtain an image of the Earth.
- **Electrical Power Supply (EPS)** consists on solar panels and batteries to provide a continuous source of power to the satellite.
- **Antenna Deployment System (ADS)** is responsible for deploying the antennas. It is used only at the beginning of the mission.

These subsystems are typical for most of the satellites, big or small. Satellites can be classified also according to their size, as presented in Table 1:

| Class                        | Mass (kg)  | Cost(\$M) |
|------------------------------|------------|-----------|
| Conventional large satellite | > 1000     | > 1000    |
| Conventional small satellite | 500 - 1000 | 25 - 100  |
| Minisatellite                | 100 - 500  | 7 - 25    |
| Microsatellite               | 10 - 100   | 1 - 7     |
| Nanosatellite                | 1 - 10     | 0.1 - 1   |
| Picosatellite                | < 1        | < 1       |

Table 1: Classification of spacecrafts by mass and cost [4].

### 2.1.1 CubeSat standard

Conventional satellites design and manufacturing time between 5 and 10 years and the cost of whole mission can be very high [4]. In recent years, efforts have been made to minimize the cost by developing smaller satellites when the requirements of the mission permit it. The size of a satellite is correlated with the cost of the mission since cost of launch is in order the mass of the satellite and, in a small satellite, the payload is usually cheaper due the lower complexity level [4].

To help the design process of a small satellite, CubeSat standard was developed in Stanford University and California Polytechnic State University. The standard was first published in 2000 and it is continuously updated after that [13]. Since then, the CubeSat Project has helped many universities that are designing or have designed a satellite of this size with a budget of less than 100,000 \$. The CubeSat standard defines different sizes of satellites which are classified into units. The basic single unit satellite (1U) has dimensions of 10x10x10 cm. CubeSats are scalable along a single axis, making possible to build ‘2U’ CubeSats (20x10x10 cm) and ‘3U’ CubeSats (30x10x10 cm) as is shown in Fig. 2.

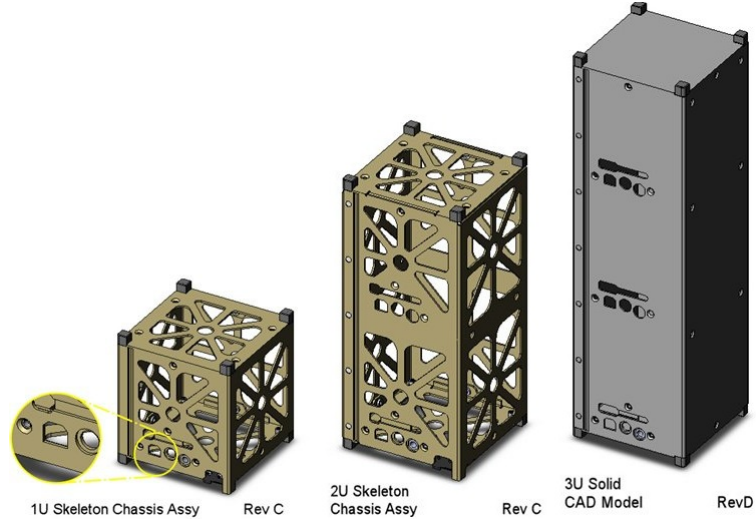


Figure 2: CubeSat sizes [14].

Life of a conventional satellite is usually several years, but for a CubeSat, lifetime can be less than one year which makes it possible save money in the redundancy and the quality of components [4]. This saving makes this area more appealing to students. And it is precisely these students that have done more work on the exploitation of the idea, although also some private companies have designed CubeSats. The knowledge produced is substantial because, despite being at a smaller scale, a CubeSat includes all subsystems already explained that a conventional satellite needs(COM, ADS, ADCS, OBC, EPS, TT&C) besides other payloads as could be a camera or other sensors.

The first CubeSats were launched in 2003 [15], and since then it has continued developing and improving the design of these small satellites. The miniaturization of electronics has helped in this work. Up to now (2013), about 50 CubeSats have been successfully launched worldwide and it is estimated that between 100 and 150 CubeSats are being developed to be launched in the next few years [10].

### Poly Picosatellite Orbital Deployer

This device, called P-POD and shown in Figure 3, is the standardized CubeSat deployment system and its aim is to house the CubeSat inside the Launch Vehicle (LV). P-POD is basically a box of anodized aluminium with the enough volume to store a 3-unit CubeSat, so it can house up to 3 ‘1U’ CubeSats. It should be noted that most of the launches in which CubeSats are sent to the space, the LV does not have only one P-POD, but several of them in the free places around a bigger satellite. [15]

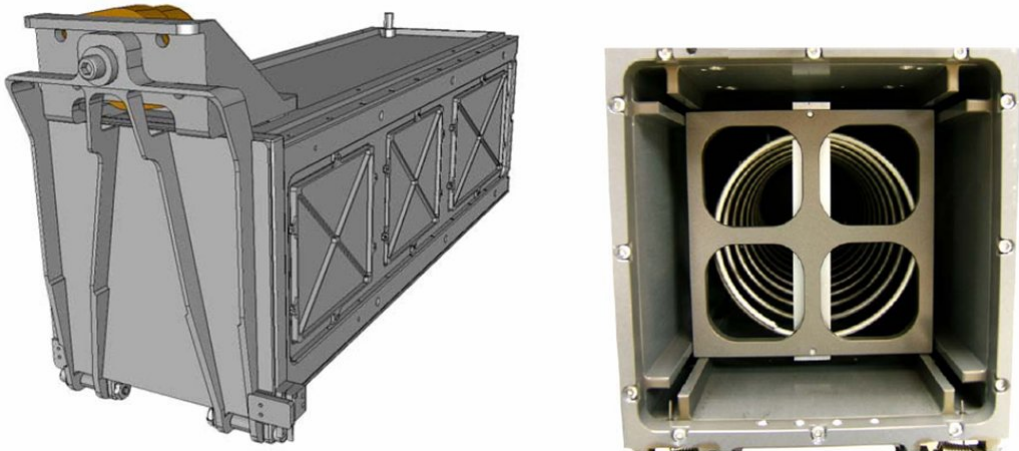


Figure 3: Poly Picosatellite Orbital Deployer (P-POD) [14].

This standard deployer limits the size of the CubeSats but, since Aalto-2 is part of the QB50 project, it also has to complain the sizes set by QB50 that appear in section 2.2.2.

#### 2.1.2 Satellite orbits

In astronomy, an orbit is the gravitationally curved path of an object around an attracting center of mass, as the Earth around the Sun or the Moon around the Earth. Planetary movements were analysed for the first time in mathematical form in the seventeenth century by Johannes Kepler. Noting the celestial mechanics of the stars, he formulated the famous three laws of Kepler, which are [4]:

- The orbit of each planet is an ellipse with the Sun occupying one focus.

- The line joining the Sun to a planet sweeps out equal areas in equal intervals of time.
- A plane's orbital period is proportional to the mean distance between Sun and the planet, raised to the power 3/2.

These three laws apply to all bodies in space, when one body is much bigger than another, and conform the called “two-body problem” in which is assumed only two objects with spherical shape that makes the gravity force exerted is modelled as if the body is a point [4]. The mathematical analysis of this problem has resulted in six parameters that completely define an orbit called the *six orbital elements* representede in Fig. 4.

Two elements define the shape and size of the ellipse [16][17]:

- Semimajor axis ( $a$ ) is the sum of the periapsis and apoapsis distances (minimum and maximum distance between the two bodies, respectively) divided by two.
- Eccentricity ( $e$ ) define the shape of the ellipse, describing how much it is elongated compared to a circle.

Another two elements define the orientation of the orbital plane in which the ellipse is embedded [16][17]:

- Inclination ( $i$ ) is the vertical tilt of the ellipse with respect to the reference plane, measured at the ascending node (where the orbit passes upward through the reference plane).
- Longitude of the ascending node ( $\Omega$ ). This parameter, horizontally orients the ascending node of the ellipse with respect to the reference frame's vernal point.

And finally [16][17]:

- Argument of periapsis ( $\omega$ ) defines the orientation of the ellipse in the orbital plane, as an angle measured from the ascending node the the periapsis.
- Mean anomaly ( $M$ ) defines the position of the orbiting body along the ellipse at a specific time. This parameter does not correspond to a real geometric angle but it can be converted into the true anomaly ( $v$ ) which does represent the real geometric angle in the plane of the ellipse, between periapsis and the position of the orbiting object.

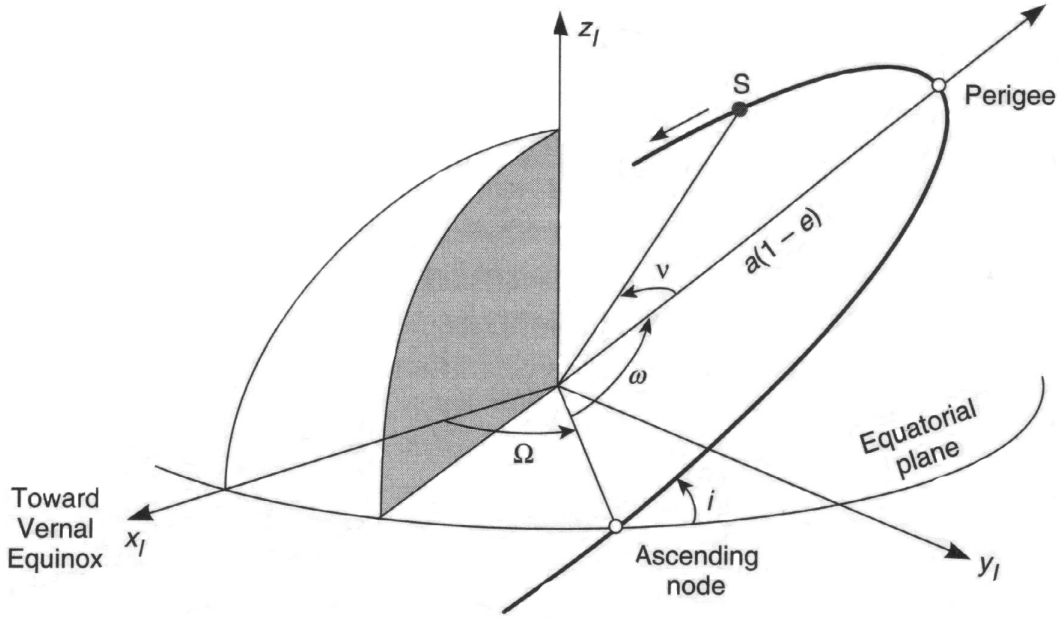


Figure 4: Characterization of an orbit and the satellite position by orbital elements [18].

There are several ways to classify the orbits but the main ones are obtained varying the first three parameters,  $e$ ,  $a$  and  $i$ .

### Orbits depending on eccentricity

Starting from a general elliptical orbit, it exists different types of relative movements between the two objects depending on  $e$ . This different trajectories are shown in Fig. 5.

- **Hyperbolic trajectories ( $e > 1$ )**. Such orbits are open orbits because the object is in an escape trajectory. The orbiting object is moving away from the second object and its velocity is greater than the escape velocity at each point of the orbit. [4]
- **Parabolic trajectories ( $e = 1$ )**. The object in this type of orbiting is characterized by having at all times the escape velocity. If energy increases, this orbit would translate into a hyperbolic trajectory. [4]
- **Elliptic and circular orbits ( $0 \leq e < 1$ )**. The ellipse is the closed orbit more general. The planets of the solar system respond to this orbit model. If the eccentricity is 0, it is possible to talk about a completely circular orbit. [4]

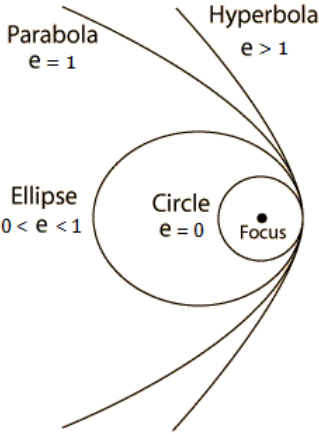


Figure 5: Orbits depending on eccentricity [19].

### Geocentric orbits

Geocentric orbits are the orbits in which the Earth is in the center of it. They are typical for many satellites and are characterized by having a quasi zero eccentricity and, for this reason, the satellites maintain at all times the distance from the Earth's surface and the relative speed to the ground. In this kind of orbits, it is possible to make a classification depending on the height (measured from the Earth's surface) and obtaining GEO, MEO and LEO orbits. They are shown in Fig. 6.

The **Gostationary Orbit (GEO)** is on the equatorial plane at a distance of approximately 36,000 km from the Earth's surface. A satellite in this orbit has a period equal to the earth rotation period and, from the point of view of the Earth, it remains fixed in the sky. Among the advantages, it is important to note that there is an uninterrupted connection which is very useful for broadcast transmission (television), but it has an excessive latency, for example, for a telephone communication. It is also very important the fact that these satellites are not visible from high latitudes. [4]

Satellites between 10,000 and 20,000 km above the Earth are in the orbit **Medium Earth Orbit (MEO)**. This is the case of the satellites for global positioning NAVSTAR-GPS, GLONASS and Galileo. The period of these satellites is about 12 hours and a constellation of satellites is needed to provide continuous coverage. [4]

Finally, the orbits with a height lower than 2,000 km are classified as **Low Earth Orbit (LEO)** orbits. These orbits are suitable for point to point communication because the transmission time is negligible. The period is around 90 minutes and the main disadvantage is the amount of time when there is direct visibility to the satellite, which is usually about 10 minutes on each pass. In addition, due to the Earth rotation, when the satellite completes an orbit, the earth has moved under-

neath and the direct communication with the base station is possible only a few minutes per day [4]. Due to the proximity to Earth, LEO satellites have a lower latency and less losses (modelled with the equation 16) and this makes that the transmission requires require less amplification.

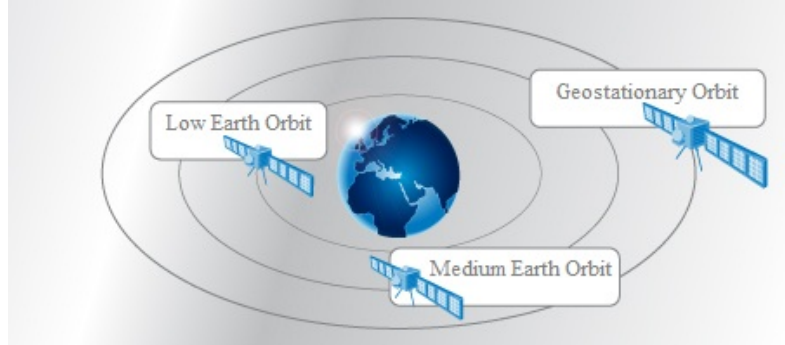


Figure 6: Geocentric orbits [20].

Aalto-2 will be orbiting in a LEO orbit and this submits limitations in communications. The biggest problem is the available time to establish a communication between the satellite and the ground. This largely depends on the height of the orbit as well as the inclination of it. To this, it is needed to add the difficulty of aiming the receiving antenna toward the satellite in the small amount of time in which it is visible. It is also important to take into account the drag of the atmosphere on the satellite that causes a gradually decrease of the orbit height, and this results in less time of communication with the satellite.

### Inclined orbits

Finally, depending on the inclination of the orbit, it is possible to differentiate between equatorial orbits, if the inclination is  $0^\circ$ , and tilted orbits. An example of equatorial orbit is the GEO orbit because if it was in a tilted orbit, it would not remain fixed in the sky. If the inclination is less than  $90^\circ$  the orbit has a prograde movement, because the satellite is revolving in the same direction as the primary body is rotating. However, if the inclination is greater the satellite will have a retrograde motion. [4]

At the same time, if the inclination is very close to  $90^\circ$ , the satellite has a polar orbit because the satellite passes above or nearly above both poles of the planet being orbited on each revolution. This kind of orbits are often used for earth-mapping taking advantage of the longitude variation the satellite see in each orbit. It is also common for polar orbiting satellites to choose a sun-synchronous orbit: meaning that each successive orbital pass occurs at the same local time of day. This can be very important for atmospheric measurements like those that will be made by the Aalto-2 satellite and for applications such remote sensing. [4]

### 2.1.3 Two-Line Elements

Two-Line Elements (TLE) is a standard satellite orbit parameter format used by North American Aerospace Defense Command (NORAD) and NASA. NORAD is an institution which keeps track of the space objects around the earth, determine their orbit and distribute their TLE freely on the Internet. With this data, a computer program can compute the position of a satellite at a particular time. [21]

The TLE of a satellite present all the information of its orbit in two lines, as the name says. The format is the following:

```

ISS (ZARYA)
1 25544U 98067A 13166.62319444 .00005748 00000-0 10556-3 0 120
2 25544 51.6483 116.0964 0010829 73.3727 265.7013 15.50799671834453

```

This TLE belongs to the International Space Station (ISS). The first line inform about the identification of the satellite as well as the time mark when the TLE was generated. More interesting is the second line which, in order, informs about the satellite number, inclination, right ascension of the ascending node, eccentricity, argument of perigee, mean anomaly, mean motion (revolutions per day) and revolution number at epoch. [21]

## 2.2 Aalto-2 satellite

Aalto-2 is a ‘2U’ CubeSat being developed by Aalto University School of Electrical Engineering in Espoo, Finland. It is also part of the QB50 program and will be one of the 50 CubeSat constellation, the first European nanosatellite network [10]. For this reason, QB50 consortium will provide the primary payload and the affordable launch for the satellite [10]. QB50 project goals and background is described in more detail in next section.

Aalto-2 team is responsible developing the satellite in schedule, besides the additional payload (optional) and the communication systems, including the ground station. The first CubeSat developed by Aalto University, Aalto-1, has proportioned knowledge in space technology to this team. Aalto-1 satellite is bigger (‘3U’ CubeSat) than Aalto-2 and more complex because of its payload, that includes a Spectral Imager (AaSI), a radiation monitor (RADMON) and a Electrostatic Plasma Brake (EPB) [9][22].

The main goals of the Aalto-2 project are the following [23]:

- To design, manufacture, and integrate the Aalto-2 satellite according to the QB50 project schedule and specifications.
- To deliver the Aalto-2 satellite to the QB50 Consortium for launch in schedule.
- To support QB50 science operations with a ground station in Otaniemi, Espoo, Finland.
- To implement additional payload for the Aalto-2 satellite.
- To use Aalto-2 satellite measurements in scientific studies.
- To generate spin-offs in Finland.
- To develop small satellite technology in Finland.
- To be a stepping stone towards a Finnish Nanosatellite Program.

In addition, the possibility of an Inter Satellite Link (ISL) is being studied by the Aalto-2 team. If finally this ISL is implemented, it will probably be between Aalto-2 and ESTELLE satellite. The latter is also part of the QB50 project and is being developed by the Estonian team at University of Tartu, Estonia.

### 2.2.1 QB50 project

QB50 program is an initiative of Von Karman Institute and its goal is the study of the lower thermosphere (90-320 km) using approximately 40 ‘2U’ and 10 ‘1U’ CubeSats that will be launched at the same time carrying the same “QB50 science payload” to make measures to the key constituents and parameters of the unexplored thermosphere as their orbit decays through it. Besides this, measurements

will be made in the re-entry process to build an improved model to predict lifetime and impact area of the satellites. [10]

The benefits associated with this project are the same that are associated with satellites in low LEO orbits. The low lifetime (3 months at maximum) reduce the cost of the satellite design considerably by not needing very high quality components which can withstand radiation produced by the Van Allen Belts. Moreover, due to the low height of the orbit, higher data rates are allowed.

All satellites will be launched at a time in a circular orbit between 350 and 400 km from earth's surface. Due to atmospheric drag, the height of the orbit will decay and this way it will be possible to make measurements at various heights in a natural way, ie, without the use of thrusters. [10]

### 2.2.2 QB50 requirements

Besides the requirements that all the CubeSats have to comply, Aalto-2 has also to comply the QB50 requirements. The requirements are specified in QB50 documentation [24]. The following four are the most important regarding the work at hand. The first one has to be taken into account when designing the antennas, and the next three are important for the communication budgets.

- **QB50-SYS-1.1.2.** In launch configuration the CubeSat shall fit entirely within the extended volume dimensions shown in Figure 7 for a ‘2U’ Cubesat, including any protrusions.
- **QB50-SYS-1.5.1.** If UHF is used for downlink, the CubeSat shall use a downlink data rate of 9.6 kbps.
- **QB50-SYS-1.5.2.** Each CubeSat carrying a set of standard QB50 science sensors shall communicate a volume of at least 2 Megabits of science data per day to the ground station that is operated by the university providing the CubeSat.
- **QB50-SYS-1.5.15.** The CubeSat shall use the AX.25 Protocol.

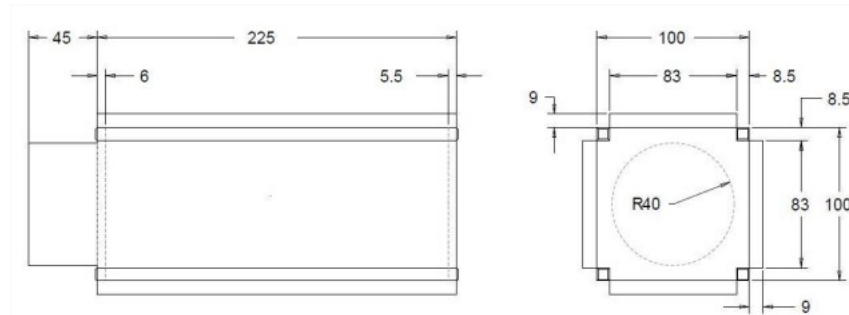


Figure 7: ‘2U’ CubeSat extended volume dimensions in millimeters [24].

## 2.3 Satellite Communication

Communication between satellites and ground station have different aspects in comparison with communications on Earth. Information travels the same way that mobile communications, carried by electromagnetic waves, but the channel is different. Whereas on Earth, the waves travel inside the atmosphere, for a satellite communication the waves have to travel through it.

Some peculiarities are related to atmospheric attenuation dependency as well as the specific protocols used for satellite communication. In this section, the most important of them are explained.

### 2.3.1 Electromagnetic radiation

Electromagnetic radiation (EMR) is the combination of both electric and magnetic fields which travel through the space oscillating and carrying energy. This behaviour was predicted by James C. Maxwell using the *Maxwell equations* developed from previously unrelated observations, experiments, and equations of electricity, magnetism and optics into a consistent theory. He demonstrated that electricity, magnetism and light are all manifestations of the same phenomenon, the electromagnetic field. [25][26]

These two field components stand in a fixed ratio of intensity to each other, and which oscillate in phase perpendicular to each other and perpendicular to the direction of energy and wave propagation. Opposite to other kind of waves, like sound, the EMR can propagate in the vacuum and does it at the speed of light. This was demonstrated in 1865 with the publication of *A Dynamical Theory of the Electromagnetic Field*. About 20 years later, in 1887, Heinrich R. Hertz could experimentally prove Maxwell's theory in his own laboratory and he realized that the speed of the waves in the air was very close to the speed predicted by Maxwell, 300,000 km/s. [25] [26]

EMR is classified according to the frequency of the oscillation. The electromagnetic spectrum, in order of increasing frequency and decreasing wavelength, consists of radio waves, microwaves, infrared radiation, visible light, ultraviolet radiation, X-rays and gamma rays. This is shown in Fig. 8.

Radio waves which are commonly used for communication have frequencies from 300 GHz to as low as 3 kHz, and corresponding wavelengths ranging from 1 millimeter to 100 kilometers. All this range was sorted by the ITU in different sub-bands showed in Table 2.

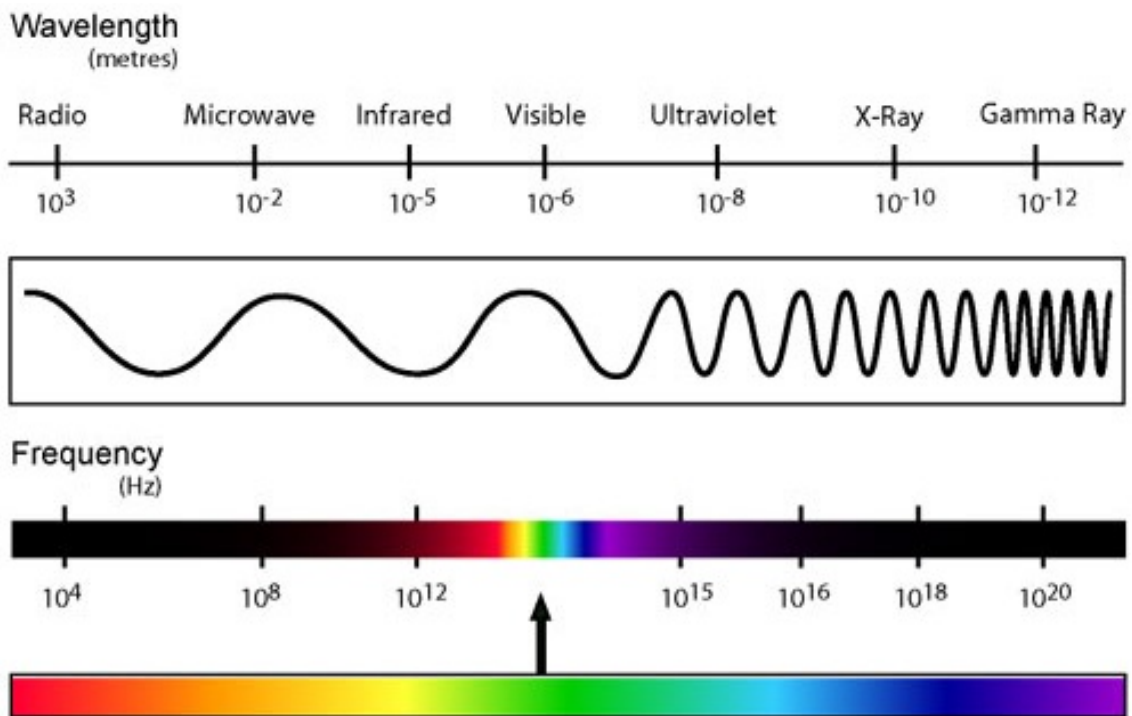


Figure 8: Electromagnetic spectrum [27].

| BAND | FREQUENCY    | WAVELENGTH   | DENOMINATION             |
|------|--------------|--------------|--------------------------|
| ELF  | < 3 kHz      | > 100 km     | Extremely Low Frequency  |
| VLF  | 3 - 30 kHz   | 100 - 10 km  | Very Low Frequency       |
| LF   | 30 - 300 kHz | 10 - 1 km    | Low Frequency            |
| MF   | 0.3 - 30 MHz | 1000 - 100 m | Medium Frequency         |
| HF   | 3 - 30 MHz   | 100 - 10 m   | High Frequency           |
| VHF  | 30 - 300 MHz | 10 - 1 m     | Very High Frequency      |
| UHF  | 0.3 - 3 GHz  | 100 - 10 cm  | Ultra High Frequency     |
| SHF  | 3 - 30 GHz   | 10 - 1 cm    | Super High Frequency     |
| EHF  | 30 - 300 GHz | 10 - 1 mm    | Extremely High Frequency |

Table 2: Radio waves sorted in bands [28].

### 2.3.2 Electromagnetic waves

As is mentioned above an electromagnetic wave is composed by both electric and magnetic fields, perpendicular to each other and also perpendicular to the direction of propagation [29]. This behaviour is illustrated in Fig. 9.

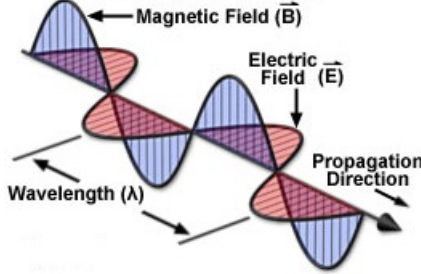


Figure 9: Electromagnetic wave [30].

The Maxwell's equations give a general solution to describe the behaviour of each one of the fields. The electrical field will be taken as example to show all the parameters that both fields have. The vector of the electric field  $\vec{E}$  can be described as follows [29]:

$$\vec{E} = \vec{E}_0 \cos(\vec{k} \cdot \vec{r} - \omega t), \quad (1)$$

where  $\vec{E}_0$  is the electric field in  $t = 0$ , the direction of  $\vec{k}$  gives the direction of propagation of the electric wave and the magnitude of  $\vec{k}$  is  $2\pi$  divided by the wave's wavelength and is related to the wave's frequency through its velocity

$$k = \frac{2\pi}{\lambda}; \quad \omega = 2\pi f; \quad f = \frac{1}{T} = \frac{c}{\lambda}, \quad (2)$$

where  $\omega$  is the wave's angular frequency,  $f$  is its frequency,  $T$  is its period,  $c$  is its speed, and  $\lambda$  is its wavelength [29].

The electrical field can also be expressed in phasorial notation using Euler's identity [29]:

$$e^{\pm j\phi} = \cos \phi \pm j \sin \phi, \quad (3)$$

where  $\phi$  is the phase and  $j$ , the imaginary unit. In this way you can express a cosine or sine, as the real or imaginary part of the exponential whose exponent is the argument of trigonometric function. Then it is possible to rewrite the equation of a wave as follows:

$$\cos \phi = \Re [e^{\pm j\phi}] \implies \vec{E} = \Re [\vec{E}_0 \cdot e^{j(\vec{k} \cdot \vec{r} + \omega t)}]. \quad (4)$$

Now, looking the vector  $\vec{E}_0$ , it is possible to define the polarization of the wave, which may be linear, elliptical or circular. This is determined by the two components of

this vector, both perpendicular to the propagation direction  $\vec{k}$  [29]:

$$\vec{E}_0 = E_{0\parallel} e^{j\theta\parallel} \cdot \vec{u}_{\parallel} + E_{0\perp} e^{j\theta\perp} \cdot \vec{u}_{\perp}, \quad (5)$$

where the term  $E_{0\parallel} e^{j\theta\parallel}$  is the magnitude and phase of the parallel component with the direction given by the vector  $\vec{u}_{\parallel}$ , and  $E_{0\perp} e^{j\theta\perp}$  and  $\vec{u}_{\perp}$  are the same but related to the perpendicular component. The motion of these terms with time give as a result so called wave polarization.

### 2.3.3 Channel characteristics

The transmission channel is the combination of the medium over which the signal must be transmitted and its properties. For satellite communications the channel characteristics vary according to the satellite orbit and the carrier frequency used. The main impairments on it are the attenuation and the addition of noise but there are more characteristics to take care of [11][31]. The most important channel characteristics are:

- **Additive White Gaussian Noise (AWGN).** This kind of noise is called additive because it just adds to the signal; white because, as the white colour, it contains all the frequencies and has a constant power spectral density, often given as  $N_0$  [W/Hz]; and gaussian because the noise amplitude probability density function is gaussian shaped. The noise power received is directly proportional to the bandwidth (BW) of the receiver. Usually, communication devices working with low frequencies also have a low band with so both parameters are directly related. If the receiver bandwidth is  $B$  [Hz], then the total noise power will be  $B \cdot N_0$  [W]. [11][31]
- **Doppler effect.** In a LEO orbit, the path loss is not a problem due to the small distance, but Doppler shift become severe. When the satellite has a relative velocity of  $v$  [m/s] along the line of sight, then the received signal has a frequency shift on it given by  $v/\lambda$ . This Doppler shift can be many times the BW of the receiver and hence requires the use of frequency tracking in the receiver. [11][31]
- **Multipath and shadowing.** Shadowing is also a major problem for satellite communications since the direct line of sight between satellite and Ground Station (GS) can be hampered by buildings or trees. For low elevation angles the problem is even bigger because the multipath is added to the shadowing. That is why it is important to add a minimum elevation parameter in the orbit simulations to calculate the available minutes per day to calculate, for instance, the data budget explained in section 2.5.2. These two effects can be modeled together in the called **fading**, which is the deviation of the attenuation affecting a signal over certain propagation media. Fading varies with time, geographical position and radio frequency used and is modelled as a random process. [4][31]

Signals from satellites in higher orbits propagate through what is essentially free space. The intensity of the signal decreases in proportion to  $1/r^2$  as the distance  $r$  from their source increases, but the signal is not disturbed until the last few kilometers. There are two layers at the atmosphere where unpredictable phenomena may affect the system performance: the ionosphere (80 - 700 km) and the troposphere (0 - 18 km). These phenomena are briefly explained below. [4]

- **Atmospheric refraction** causes a slight shift in the apparent elevation of the satellite. The magnitude of the shift depends on the elevation as well as on the atmospheric pressure and water vapour content. [4][31]
- **Attenuation** in the troposphere has two causes. The first is molecular absorption by gases such as oxygen and water vapour. Both gases have strong absorption bands at 60 GHz and 22.2 GHz, respectively, which are used for remote sensing applications. Much more dramatic attenuation effects are caused by rain. Water droplets both scatter and absorb radiation, the effect being strongest when the drop size is of the order of a wavelength. [4][31]
- **Scintillation**, or rapid fluctuation in signal amplitude analogous to the twinkling of stars, is normally a small effect that for most purposes can be ignored. However, at low elevations, because of the longer atmospheric path, it can not be neglected. [4][31]
- **Depolarization** of the signal is another consequence of rain. Because rain-drops are slightly flattened, they absorb one plane of polarization rather more than the other. Depending on the inclination shift between the axis of the drops and the plane of polarization of the signal, rain drops also causes a slight rotation of the plane, or in the case of a circularly polarized signal, a slight ellipticity of polarization. Fortunately, the resulting power loss due to mismatch between the signal polarization and that of the receiving antenna is not significant. [4][31]

All the effects above explained are unavoidable except those dependent on the frequency. Losses due to atmospheric gases (Nitrogen, Oxygen, Carbon Dioxide, Hydrogen, etc.) are nearly independent of atmospheric temperature, mean density and relative humidity at frequencies below 2 GHz and that is why the band used by the Aalto-2 (UHF) is used by most of the CubeSat missions. Atmospheric absorption depends strongly upon the total number of molecules distributed along the path between the spacecraft and the ground station. This, in turn, means that the losses from or to the satellite are elevation angle dependent. Table 3 shows the relationship between elevation and absorption losses at the troposphere. [25]

| Elevation angle | Loss (dB) |
|-----------------|-----------|
| $0^\circ$       | 10.2      |
| $2.5^\circ$     | 4.6       |
| $5^\circ$       | 2.1       |
| $10^\circ$      | 1.1       |
| $30^\circ$      | 0.4       |
| $45^\circ$      | 0.3       |
| $90^\circ$      | 0         |

Table 3: Loss due to atmospheric gases [25].

### 2.3.4 Protocols

To establish a communication, protocols are necessary. A communication protocol is a set of rules that permit the correct data transmission between two entities. It comes to the rules or the standard, that defines the syntax, semantics and synchronization of the communication as well as possible methods to correct errors in it. [32]

In telecommunications' field, it is common to list protocols in seven levels, using so called OSI (Open Systems Interconnection) model, developed by the International Organization for Standardization (ISO) in 1983 and revised in 1995 [32]. This model consists in seven layers exposed in Table 4.

| Layer           | Function  |
|-----------------|---|
| 7. Application  | Network process to application                                  |
| 6. Presentation | Data representation, encryption and decryption                  |
| 5. Session      | Interhost communication, managing sessions between applications |
| 4. Transport    | End-to-end connections, reliability and flow control            |
| 3. Network      | Path determination and logical addressing                       |
| 2. Data link    | Physical addressing   |
| 1. Physical     | Media, signal and binary transmission                           |

Table 4: OSI model [32].

For the Aalto-2 mission is important to explain in detail the protocols used at the first four levels because these are the influential layers for the data budget calculation at section 4.1.3. At QB50 documentation it is specified the use of AX.25 protocol but there is no requirement yet (June, 2013) for the transport layer. Now, AX.25 and the most known and used transport protocols will be explained.

### AX.25

This protocol is designed for use by amateur radio operators and is very extensively on amateur packet radio networks. AX.25 occupies the first, second and often the

third layers of the OSI networking model, and is responsible for transferring data between nodes and detecting errors introduced by the communication channel. Its version 2.0 was released in October, 1984 and has been in use since late 80's. The last stable version, 2.2, was released in 1998. [33]

The data at the link-layer is transmitted in small blocks of data called frames. These frames have property to be sent in a connection-oriented as well as connectionless service mode. In connection oriented mode, a connection must be established between source and destination before the data transfer starts. Instead, when the transmission of data is done in a connectionless mode, it is possible sending messages to other hosts without prior communications to set up the channel. [33]

### Transport protocols

Transport Control Protocol (TCP) is the most well-known transport protocol for the radio amateurs. This protocol performs error control, retransmission of corrupt packets, ack's system and connection-oriented transmissions [32]. The size of the TCP overhead is 20 bytes. Applications that do not require the reliability of a TCP connection may instead use UDP protocol. Because the extended use of TCP in all kind of communications and the high probability that Aalto-2 mission has to use it, its header is shown in Table 5.

User Datagram Protocol (UDP) is a connectionless protocol where the messages are referred as datagrams. Due to the connectionless mode, there is no guarantee of delivery, ordering or duplicate protection but UDP provides checksums for data integrity [32]. This protocol is suitable for purposes where error checking and correction is either not necessary, avoiding the corresponding overhead, which in this case has a size of 8 bytes.

Reliable User Datagram Protocol (RUDP) is an evolution of UDP which includes datagram ordering at the reception point as well as reliability but with less overhead and complexity than TCP protocol. The features added to UDP to achieve this are: acknowledgement of received packets, windowing and flow control, retransmission of lost packets and over-buffering (faster than real-time streaming) [34]. Even with all these new features, the overhead added to the information is 6 bytes.

| 1                      |     | 2     |    | 3                |    | 4  |    |  |  |  |  |
|------------------------|-----|-------|----|------------------|----|----|----|--|--|--|--|
| 0                      | 1   | 2     | 3  | 4                | 5  | 6  | 7  |  |  |  |  |
| 8                      | 9   | 10    | 11 | 12               | 13 | 14 | 15 |  |  |  |  |
| 16                     | 17  | 18    | 19 | 20               | 21 | 22 | 23 |  |  |  |  |
| 24                     | 25  | 26    | 27 | 28               | 29 | 30 | 31 |  |  |  |  |
| Source port            |     |       |    | Destination port |    |    |    |  |  |  |  |
| Sequence number        |     |       |    |                  |    |    |    |  |  |  |  |
| Acknowledgement number |     |       |    |                  |    |    |    |  |  |  |  |
| Offset                 | Rvd | Flags |    | Window size      |    |    |    |  |  |  |  |
| Checksum               |     |       |    | Urgent pointer   |    |    |    |  |  |  |  |

Table 5: TCP header.

## 2.4 Antennas

The Institute of Electrical and Electronics Engineers (IEEE) define antenna as the part of a transmission or receptor system specifically designed to radiate or receive electromagnetic waves. The goal of the antenna is to radiate the power provided with the directionality characteristics suitable for the application. [35]

Antennas are a very important part of the design of a satellite since most space-craft communication links are made by them. Transmitters and receivers are quite straight-forward devices (in link modelling terms); antennas are not. They have characteristics of impedance and radiation which depend on the frequency. Because they will be part of a larger system, it is interesting to characterize these parameters to assess the effect of a particular antenna in a system. These parameters are detailed below. [35]

### 2.4.1 Impedance

The antenna is directly connected to a transmitter and its goal is to radiate the maximum power while minimizing losses. At the entrance of the antenna, the input impedance  $Z_A$  is defined using voltage-current relationships. Generally, this one has real part  $R_A(\omega)$  (resistance) and imaginary part  $X_A(\omega)$  (reactance) both depending on the frequency. If the latter is zero, it is achieved a resonant antenna. [35]

Because antenna radiates energy, there is a net power loss due to this fact. To model this behaviour of the antenna, is possible to assume a radiation resistor  $R_r$  that would be which ohmically dissipates the same power as radiated by the antenna. On the other hand, the potential losses will be assigned to so called losses resistor  $R_\Omega$ . Thus it is possible to define the power delivered to the antenna as the sum of the radiated power and lost power. [35]

$$P_{delivered} = P_{radiated} + P_{lost} = I^2 R_r + I^2 R_\Omega, \quad (6)$$

where  $P$  denotes power and  $I$  is the electric current. Furthermore, the relationship between the radiated power and the delivered one defines the called *antenna efficiency*  $\mu_l$  [35], defined as

$$\mu_l = \frac{P_{radiated}}{P_{delivered}} = \frac{R_r}{R_r + R_\Omega}. \quad (7)$$

### 2.4.2 Radiation pattern

A radiation pattern is a graphical representation of the radiation properties of the antenna as a function of the directions in space. Normally, a spherical coordinate system to define the radiated power as a function of the angular variables  $(\theta, \phi)$  is used. Thus it is possible to represent a three-dimensional diagram and express the power levels in dB in relation to the maximum of radiation. Figure 10 is an example of this kind of representation. [35]

Often, it is enough to represent a section of the three-dimensional diagram maintaining fixed the angles  $\theta$  or  $\phi$ . The most common practice is the use of polar or cartesian coordinates. In these representations is easier to appreciate the different parts of the diagram, such the area in which the radiation is maximum called main lobe besides the adjacent areas where other relative maximum are, called side lobes. In addition, seeing the plot, it is possible to define a few important parameters. [35]

- The beamwidth ( $\Delta\theta_{-3dB}$ ) of an antenna is typically taken to be twice the angle between the boresight (direction of maximum power) and the direction where the power has a roll-off value of a factor of 2 (that is, -3 dB).
- The side lobe level (NPLS) is the ratio, in dB, between the values of the main lobe and the side lobe.
- If the radiation pattern presents revolution symmetry, it is said the antenna is omnidirectional.

Isotropic antenna is called to an ideal antenna that radiates the same intensity of radiation in all directions of space. Although there is no antenna with these characteristics, it is very helpful to express the directivity parameter of an antenna. [35]

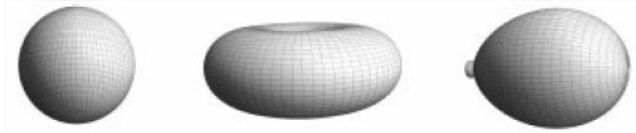


Figure 10: Isotropic, omnidirectional and directive radiation patterns [35].

#### 2.4.3 Directivity and gain

The *directivity* (D) of an antenna is a measure of how the antenna concentrates the transmitter's power in a particular direction in relation to some coordinate system fixed on the antenna. The directivity of a highly directive antenna is typically taken to be the peak value (sometimes called the boresight directivity). It is usually measured as the ratio of the power directed in the peak direction divided by the same power when it is radiated isotropically (i.e., equally in all directions). An example to illustrate this concept would be the next one: an isotropic antenna has directivity 1 but if the antenna radiates uniformly only in one hemisphere, the directivity would be 2 and if it only do it in one octant, would be 8. [35]

Some antennas will have losses (explained in section 2.4.1) associated with getting the power from the antenna input to the radiating element. The *gain* (G) of an antenna is the directivity (measured in dB above an isotropic radiator [dBi]) minus the antenna feed losses (also measured in dB). For satellite systems operating in the amateur satellite service the term gain is more frequently used and is related to the directivity by the parameter antenna efficiency  $\mu_l$ . [35]

#### 2.4.4 Polarization

Polarization of an antenna is, in fact, the study of the polarization of the waves that it radiates. It is possible to change the parameters of the wave's equation making the antenna to radiate waves with a certain behaviour. The purpose of this may be, for example, the proper adaptation with the receiving antenna or the prevention of losses when the information is travelling. Continuing from the exposed above in section 2.3.2, the direction of propagation will be along the  $z$  axis and the components of the vector  $\vec{E}_0$  will be the  $x$  and  $y$  axis. [35]

Thus, both the complex vector  $\vec{E}_0$  and  $\vec{E}$  when  $z = 0$  will have a generic expression as follows:

$$\vec{E}_0 = \hat{x}Ae^{j\theta_A} + j\hat{y}Be^{j\theta_B}; \quad \vec{E} = \hat{x}A \cos(\omega t + \theta_A) - j\hat{y}B \sin(\omega t + \theta_B), \quad (8)$$

where  $A$  and  $B$  are real constants and  $\theta_A$  and  $\theta_B$  are its respective phases. Table 6 shows the different possible polarizations and the conditions that must be met for each. [35]

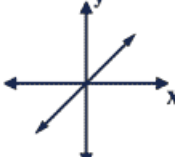
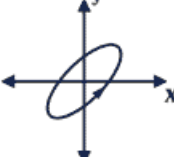
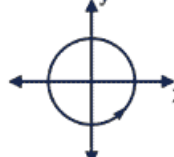
| Polarization | Linear  | Elliptical   | Circular  |
|--------------|---|--|---|
| Conditions   | $A = 0, B \neq 0$ or $A \neq 0, B = 0$<br>$ \theta_A - \theta_B  = n\pi$            | $0 \neq A \neq B \neq 0$<br>$ \theta_A - \theta_B  \neq 0$                           | $A = B$<br>$ \theta_A - \theta_B  = (2n - 1)\frac{\pi}{2}$                            |
| Example      |  |  |  |

Table 6: Linear, elliptical and circular polarization [36].

#### 2.4.5 Bandwidth

All antennas, due to their finite geometry, are limited to operate successfully in a band or frequency range. This interval, the bandwidth of an antenna, is the range of frequencies over which the antenna maintains certain required impedance, pattern or polarization characteristics. The value of this parameter will be imposed by the system and will affect the more sensitive or critical parameter of the application which, for electrically small antennas having dimensions less than about a half-wavelength, is the impedance variation. [35]

#### 2.4.6 Antenna matching

The antenna is connected to a transmission line or directly to a receiver. To have maximum power transfer, the impedance of the antenna  $Z_A = R_A + jX_A$  and the

load impedance  $Z_L = R_L + jX_L$  must be complex conjugate  $Z_L = Z_A^*$ . Thus, the resulting reactance would be null and, this way, the resonance point of the antenna, i.e., the point of maximum power transfer, would be achieved. In case of fail,  $C_a$  is defined as the mismatch coefficient and it is expressed as follows:

$$C_a = \frac{4R_a R_L}{(R_A + R_L)^2 + (X_A + X_L)^2}, \quad (9)$$

where  $R_A$  and  $X_A$  are the resistance and reactance of the antenna, and  $R_L$  and  $X_L$  are the resistance and reactance of the load. [35]

#### 2.4.7 Effective area

The power available from a loss free antenna is the product of the power flux per unit area, and the effective aperture area of the receiving antenna ( $A_R$ ) [11]. Calculating this area is easy for antennas with a surface measurable such as the parabolic antennas, but for monopoles and dipoles this is impossible. At this point is when the concept of *effective area* appears which depends on the gain of the antenna and permit to calculate the incoming power. The relationship between effective area and gain is given by the formula:

$$A_R = \lambda^2 G_R / 4\pi, \quad (10)$$

where  $A_R$  and  $G_R$  are the effective area and the gain of the receiving, respectively [37].

It is clear to see in the formula, that effective area has a direct relationship with the wavelength. This means that if two antennas have the same gain, the antenna working in a lower frequency (longer wavelength) will be bigger in physical dimensions. This, for parabolic antennas, has the consequence of the increase of the diameter and for dipoles and monopoles, the increase of the length of them.

## 2.5 Communication budgets

The satellite has to send the information captured by its sensors to the GS for analysis. To assure the correct data transmission, two budgets have to be calculated: the link budget and the data budget. But first of all, it is good to know the three categories in which data transmitted between satellite and GS can be divided. These are the beacon, the telemetry and the telecommands [4].

### Beacon

The beacon is a simple radio signal generated by the satellite in order to inform any listener about its identification and position. This is the only signal that Sputnik-1, the first artificial satellite, was able to transmit due to its easiness of implementing. Beacon has more application than the one for identification, it is also used to adjust the GS's output power depending on the strength of the signal received as well as detect de Doppler shift in order to tune the GS compensating it. [4]

### Telemetry

Telemetry data, as the beacon, is sent from the satellite to the GS and can be divided in three sub-categories as follows [4]:

- *Housekeeping data* informs about the operating status of all the subsystems on board the satellite like pressures, temperatures of the components, voltages, currents, etc.
- *Attitude data* is the data generated by all the attitude sensors that satellite carries such as magnetometers, accelerometers, gyroscopes and Sun, Earth and star sensors.
- *Payload data* is the most important data generated by the satellite. This data is the reason why the satellite has been developed. It can be since the composition of the atmosphere, until a picture of the Earth. The payload data is different in every mission and has to be considered individually.

### Telecommands

Telecommands are orders that GS sends to the satellite in order to control its functions and achieve a desirable behaviour. for relatively simple missions there are three basic types of commands, as follows [4]:

- *Low-level on-off commands*. These are logic-level pulses used to set or reset bi-stable logic.
- *High-level on-off commands*. These commands are higher-powered pulses, capable of operating a latching relay or RF waveguide switch directly.

- *Proportional commands.* These are complete digital words, which may be used for purposes such as the reprogramming of memory locations or for setting up registers in the attitude control subsystem.

It is necessary to know the amount of energy for the successful transmission. The incoming power depends on the satellite solar panel attitude and the energy needed by payload influences the outgoing power and the stored energy.

### 2.5.1 Link budget

When designing a complete, i.e. end to end radio communications system, it is necessary to calculate the link budget. Link budget calculates the total effect of factors such as the required antenna gain levels, noise factors, radio transmitter power levels, atmospheric losses, cable losses, and receiver sensitivity figures. By assessing the link budget, it is possible to design the system so that it meets its requirements and performs correctly without being over-designed at extra cost. [4]

Link budgets are often used for satellite systems. In these situations it is crucial that the required signal levels are maintained to ensure that the received signal levels are sufficiently high above the noise level to ensure that signal to noise levels or bit error rates are within the required limits. In addition to satellite systems, link budgets are also used in many other radio communications systems. For example, link budget calculations are used for calculating the power levels required for cellular communications systems, and for investigating the base station coverage. [4]

A link budget is the addition and subtraction of gains and losses within an RF link. When these gains and losses of various components are determined and summed, the result is an estimation of end-to-end system performance [4]. This way, based on this result one can have estimates on how much power is necessary to produce for the RF signal in order to have a reliable communication link. In essence the link budget will take the form of the equation below [4]:

$$\text{Received power} = \text{Transmitted power} + \text{Gains} - \text{Losses} \quad (11)$$

The definition of antenna gain implies that a transmitter with output power  $P_T$  associated with an antenna of gain  $G_T$  can be replaced, for the purpose of this calculation, by an isotropic radiator with output power  $P_T G_T$ . This quantity is known as the Equivalent Isotropic Radiated Power (EIRP) [4]. From an isotropic radiator, this power would spread out uniformly so that the Power Flux Density (PFD) at a distance  $r$  from the source is

$$\text{PFD} = P_T G_T / (4\pi r^2). \quad (12)$$

If atmospheric attenuation results in power loss by a factor  $L_A$ , then

$$\text{PFD} = P_T G_T / (4\pi r^2 L_A). \quad (13)$$

Now, multiplying the effective area of the antenna (equation 10) and the power flux density, the signal power  $S$  at the input to the receiver is

$$S = P_T G_T G_R (\lambda / 4\pi r)^2 (1/L_A). \quad (14)$$

Finally for a system temperature  $T_{sys}$  the noise power density referred to the receiver input is  $kT_{sys}$ , giving a signal-to-noise-power-density ratio of

$$S/N_0 = P_T G_T (\lambda / 4\pi r)^2 (1/L_A) (G_R / T_{sys}) (1/k). \quad (15)$$

In this expression, which is known as the *telecommunications link budget equation*, the factor  $P_T G_T$  can be regarded as a figure of merit for the transmitter and the term  $G_R / T_{sys}$  as a figure of merit for the receiving system [4]. Leaving aside the constant  $1/k$ , the remaining factors refer to the propagation path. The quantity

$$L_S = (4\pi r / \lambda)^2 \quad (16)$$

is known as the *free-space loss* and, assuming a LEO satellite, it varies as the path length increases or decreases depending on the elevation of the satellite as viewed from the ground station. In terms of the space loss,  $S/N_0$  is given by

$$S/N_0 = P_T G_T (1/L_S) (1/L_A) (G_R / T_{sys}) (1/k). \quad (17)$$

Since the required  $S/N_0$  can be determined from the system specifications, this expression allows us to calculate the required transmitter power,  $P_T$ , as well as other important parameters. [4]

In communications is very common to present the link budget in two different ways. The first one is a way to normalize the result for any data bit rate referring the noise power density, not to the signal power, but to the energy per bit  $E_b$ . The second one takes care of the noise that affects the communication which is only the one who passes the bandpass filter of the receiver with a bandwidth of  $B$  Hz. Then, the noise power that affects the signal is the noise power density  $N_0$  multiplied by  $B$ . This method shows the relationship between this two powers and is called *signal to noise ratio* (SNR). Both ways to define the link budget are related by the equations

$$S = E_b R_b, \quad N = N_0 B \quad \Rightarrow \quad \frac{S}{N} = SNR = \frac{E_b}{N_0} \cdot \frac{R_b}{B}, \quad (18)$$

where  $R_b$  is the bit rate and  $N$  the noise power. [4]

### 2.5.2 Data budget

As well as the link budget have to be calculated to know the necessary transmission power for a reliable communication, a data budget is also needed. This budget will permit to know how much data is possible to transmit between satellite and GS. For this calculation, a simulation of the available minutes per day in those the satellite is visible from the GS is a fundamental parameter. It is also very important to know the size of the frame as well as the fields which conform it, which generally are [11]:

- **Overheads.** The bytes included here are not useful data of the mission. But they are necessary in order to have a reliable information transmission.
- **Telemetry.** Here, information such as the position, temperature, battery status and also the status of all the subsystems, is included.
- **Payload data.** This information is referred as all the data generated by the payload of the satellite such as images, remote sensing measurements...

Once these parameters are known it is possible to calculate the available time per day to transmit data from the payload, making possible to adjust certain parameters of them. For example, talking about an Earth observing satellite, to make the data budget will determine the amount of images which it will be possible to transmit to the GS per day. This way, an excessive picture taking is avoided.

### 3 Simulation tools

In this chapter, the three different tools used to perform the study about the communications of the Aalto-2 satellite will be presented. These tools are Satellite Tool Kit (STK), CST studio and AMSAT-IARU Link Model. The first one has been used to simulate the orbit of the Aalto-2 with the parameters given by QB50 project. The second one has been used to find the best configuration of the antennas and then, optimize it. Finally, the last one has been used to assure that it is possible to establish a communication with the satellite.

#### 3.1 Satellite Tool Kit

The simulations are done with the software STK v10, provided by Analytical Graphics, Inc (AGI). This software is very useful to analyse some different issues related with ground, air, sea and space. At the core of STK is a geometry engine that determines the time-dynamic position and attitude of the assets. When this software was created was mostly to solve problems involving Earth-orbiting satellites, but nowadays this software is used not only for that, but for both aerospace and defence communities. [38]

The possibilities of this software are endless. Just to mention a few features of it, it can be used to design a satellite constellation, to know the elapse of time in which the solar cells of the satellite are affected by sun light, and to know the available connexion time between the satellite and its ground station. [38]

#### 3.2 CST Studio

CST Studio is an electromagnetic simulation software developed to design and optimize devices operating in a wide range of frequencies. analyses may include thermal and mechanical effects, as well as circuit simulations. The software is a set of many tools, each one designed for a particular purpose such as the study of: high/low frequency devices, free moving charged particles, cable harnesses and signal integrity on printed circuit boards. [39]

The antennas of the Aalto-2 have been simulated and optimized with the module CST Microwave Studio, designed for a fast and accurate 3D-simulation of high frequency devices and time domain simulation. [39]

### 3.3 AMSAT-IARU Link Model

This tool is an spreadsheet table developed by Jan A. King for the Radio Amateur Satellite Corporation (AMSAT) and the International Amateur Radio Union (IARU). This tool is used in almost all the CubeSat missions and it is constantly improved and updated. The version used for link budget calculations in this work is the version v2.5.3. This tool is composed of all the elements which affect somehow the gains or losses that exist in a communication link ordered in different and clear tabs.

Since the path loss is the most important loss in a satellite link, it is very important to select the correct orbit that can be chosen in the first tab. Then, the frequency is selected as well as the characteristics of the transmitters and receivers. The next tabs are related with the antenna characteristic and the atmospheric losses. Finally, in the last tab, the modulation method can be selected in order to know the required strength of the signal in order to have a good communication.

## 4 Aalto-2 communication link and antenna design

Here are presented the results of the study carried out separated in two parts. Theory explained in section 2 is used with this purpose. In the first part, it can be found the calculation for both data and link budget, followed by the design of the ADS of the Aalto-2 satellite, presented in section 4.2.

### 4.1 Communication budgets calculation

In this section, communication budgets will be calculated. Link budget is very straight-forward and depends only on the orbit of the satellite and the characteristics of the transmitter and receiver. Instead, data budget depends not only on the orbit, but also the protocols used to establish the communication.

To calculate the data budget, the frame configuration is needed in order to know the length of the frame and how much of it is occupied by protocol headers. This way, it is possible to calculate the data throughput for each of the three transport protocols studied. Then, the different kinds of data that the satellite has to transmit have to be separated to know the available bytes for possible satellite payloads.

#### 4.1.1 Protocol stack and frame configuration

For this specific mission, it is important fulfil the requirements imposed by QB50 consortium specified in section 2.2.2. As is specified, the bit rate will be 9,600 bps and the use of AX.25 is mandatory. The Aalto-2 team has decided that after the 6 bytes for preamble and synchronization, the length of the AX.25 packet will be 256 bytes and a low overhead scheme (8.2%) is selected. That means Aalto-2 has 235 bytes of payload for upper layers. The next protocol to be used is not defined in the QB50 requirements yet, so there are at this point, the option to use TCP, RUDP or a modification of the TCP protocol explained below.

#### Modified TCP (M-TCP)

Some modifications can be done in the scheme of the TCP header to have more bytes for data. The idea is to maintain the advantages of TCP protocol (reliability, error checking and retransmission) but reducing the overhead taking advantage of the situation. TCP is thought for a big network that involves thousands of devices and high volumes of data. In the case studied in this paper, there will be only two active devices sending information to each other. The modifications are explained as follows:

- The original size of the fields “source port” and “destination port” is 2 bytes but these are thought for a big network. Since there are only two devices that need to be connected, 1 byte per field will be enough.

- The length of the “sequence number” and “acknowledge number” can be reduced, as well, from 4 to 2 bytes. This is possible because the satellite will not send more than  $2^{16}$  (65,334) packets in each pass over the ground station.
- The last modification that can be done is related with the “urgent pointer” field. This field is a mark in the packet that inform the receiver about the urgency that has the packet to be processed. In this case, all the packets will have the same level of importance and that is why this field can be deleted having more free space for data.

If all this modifications are possible, a 12 bytes header can be achieved. It would maintain the same procedures and advantages of normal TCP, but reducing of almost half the size of overhead. The consequence is a 3.4% increase in the data that TCP encapsulates. If finally this schema is used for the Aalto-2, it shall be published to make able the radio amateurs to decode the data. Header of the M-TCP would be as in Fig. 11.

| Bits Offset | Bits 0-3              | 4-7 | 8-15             | 16-31           |             |          |                  |                  |                  |                  |                  |                  |                  |                  |
|-------------|-----------------------|-----|------------------|-----------------|-------------|----------|------------------|------------------|------------------|------------------|------------------|------------------|------------------|------------------|
| 0           | Source Port           |     | Destination Port | Sequence Number |             |          |                  |                  |                  |                  |                  |                  |                  |                  |
| 32          | Acknowledgment Number |     |                  |                 | Data Offset | Reserved | C<br>W<br>R<br>E | E<br>C<br>E<br>G | U<br>R<br>G<br>G | A<br>C<br>K<br>K | P<br>S<br>H<br>H | R<br>S<br>T<br>T | S<br>Y<br>N<br>N | F<br>I<br>N<br>N |
| 64          | Window Size           |     |                  |                 | Checksum    |          |                  |                  |                  |                  |                  |                  |                  |                  |
| 96/192+     | Free for Data         |     |                  |                 |             |          |                  |                  |                  |                  |                  |                  |                  |                  |

Figure 11: Modified TCP Header.

Must to be clarified that M-TCP is only a theoretical protocol not implemented due to time limitations. Nowadays (June, 2013), the use of this protocol is not possible but it has been taken into account in the data budget to know its performance.

### Frame configuration

Figure 12 shows the composition of a frame for communication between satellite and ground station. The first strip is the physical layer frame, composed by an AX.25 frame plus the preamble and the synchronization field. The second strip is an AX.25 frame, composed by overhead and payload. That payload is a Protocol Data Unit (PDU) of the upper transport layer which in turn can be filled with three transport protocols already explained. The real data that will be exchanged between satellite and GS will be placed after the overhead of the transport protocol and is shown in Fig. 13.

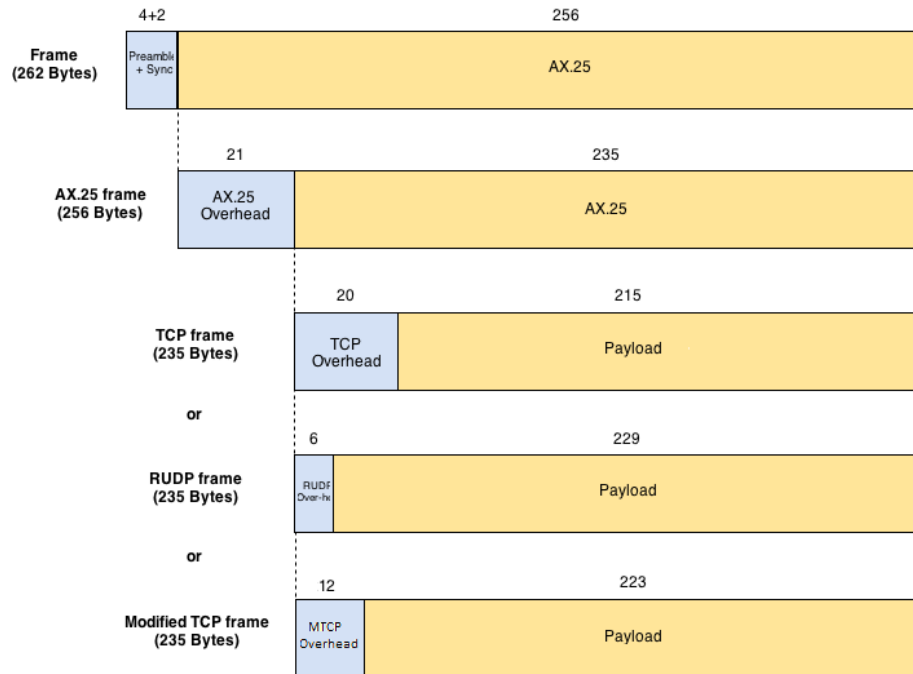


Figure 12: Frame structure per layer, with three options in the transport layer.

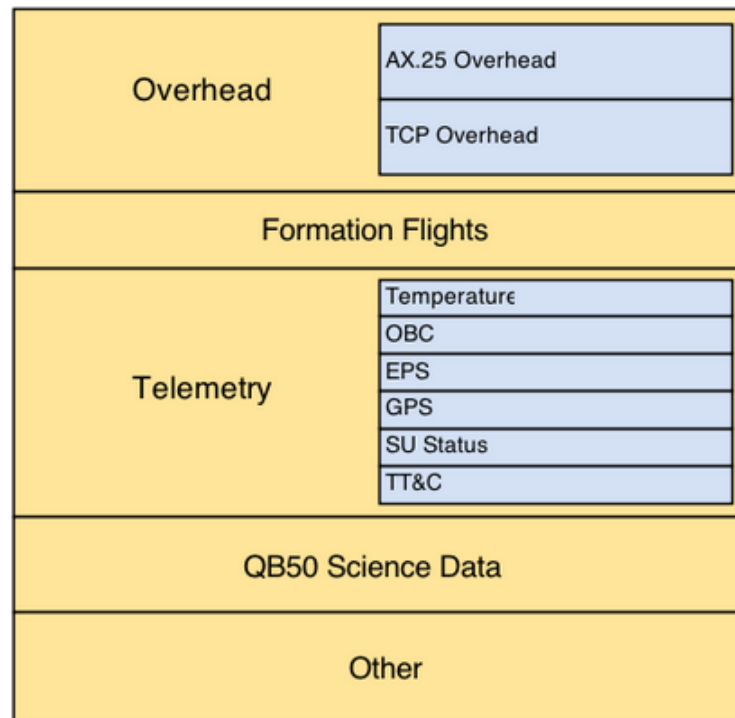


Figure 13: The communication frame sorted by field.

## Data throughput

The 9,600 bps bit rate means that 4.58 frames will be sent every second. Data throughput calculations can be done for each one of the three options at the transport layer presented above. These results are compared Table 7.

|                | TCP                   | RUDP                   | Modified TCP           |
|----------------|-----------------------|------------------------|------------------------|
| Overhead (bps) | 732.8 (20B)           | 195.84 (6B)            | 439.68 (12B)           |
| Payload (bps)  | <b>7877.6</b> (215 B) | <b>8390.56</b> (229 B) | <b>8170.72</b> (223 B) |

Table 7: Throughput at transport layer per protocol

### 4.1.2 Aalto-2 orbit and link time simulations

Simulations with STK is an important step for the data budget calculation. The goal of this simulation is to know the amount of minutes available in which there is direct sight between satellite and GS to have a communication. The parameters needed for the simulation are given by the QB50 project and nowadays are [24]:

- Sun-synchronous circular orbit. Local descending node at 11 am
- Height: 350 – 400 km
- Inclination: 98.6°

Along with this parameters, to know when it is possible to communicate with the satellite, it is necessary to determine the position of the GS which is at the roof of the ELEC building( $60^{\circ}11'19''$ ,  $24^{\circ}49'50''$ ), Otaniemi, Espoo, Finland. Both satellite and GS are shown in Fig. 14.

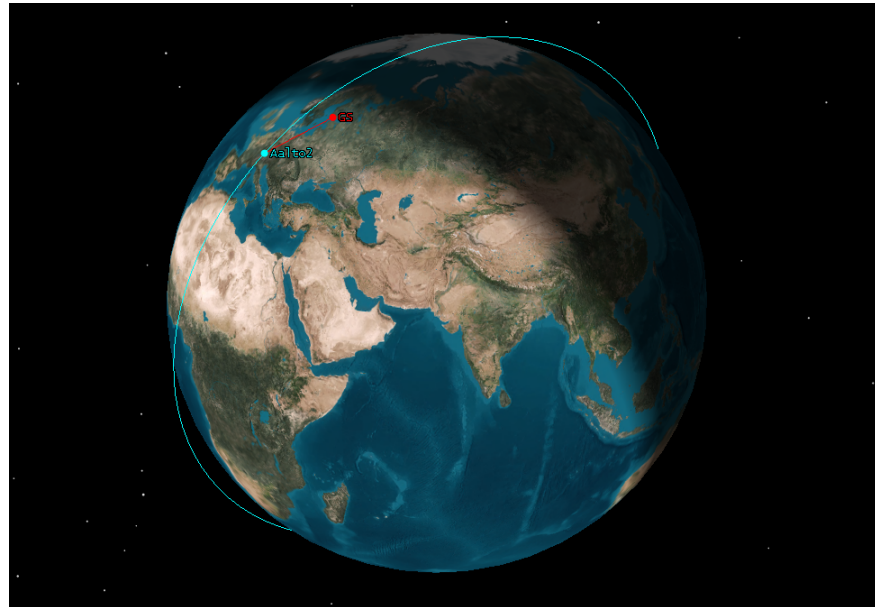


Figure 14: The Aalto-2 satellite and the ground station simulated with STK.

In STK it is possible to set a mask for the elevation in order to count the time when there is direct sight between satellite and GS only when the satellite is  $x$  degrees over the horizon seen from the GS. Table 8 shows the available time to transmit when the satellite is at the beginning of the mission depending on the minimum elevation selected in the elevation mask.

| El         | Magnitude            | 350 km       | 375 km       | 400 km       |
|------------|----------------------|--------------|--------------|--------------|
| $5^\circ$  | # passes per day     | 5.74         | 6.00         | 6.19         |
|            | Mean duration (s)    | 343.75       | 357.59       | 374.25       |
|            | Total duration (min) | <b>32.90</b> | <b>35.76</b> | <b>38.63</b> |
| $10^\circ$ | # passes per day     | 4.32         | 4.58         | 4.74         |
|            | Mean duration (s)    | 270.73       | 281.43       | 296.15       |
|            | Total duration (min) | <b>19.50</b> | <b>21.49</b> | <b>23.41</b> |

Table 8: Available connection time per day in high orbits as a function of minimal contact elevation (El).

The altitude of the satellite will decrease due to drag of the atmosphere and this is the reason to make simulations also at lower heights. To have a realistic ones, a minimum elevation of 10 degrees has been chosen to assure than possible obstacles such as trees and buildings do not make the results more optimistic than the reality will be. In Figure 15 is possible to observe the area where is possible to see the satellite and also the different paths of the satellite at different passes over the Earth.

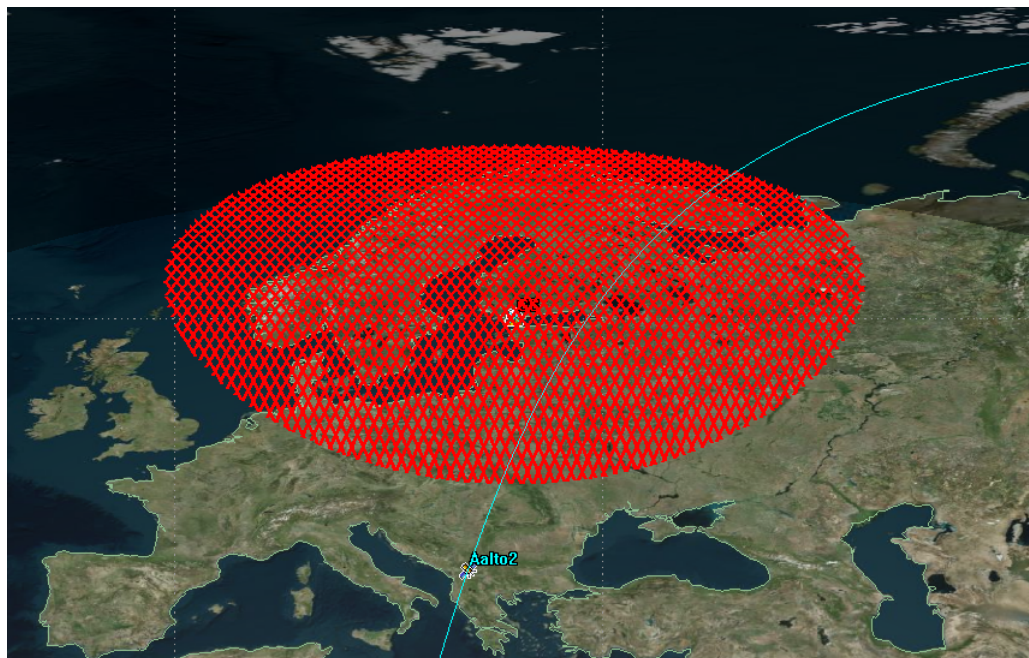


Figure 15: Available area for communications.

The results of the simulations are compared in Table 9 and will be an useful data to adjust the frame configuration during the mission lifetime as is exposed in section 4.1.3.

| Magnitude            | 300 km       | 200 km      | 100 km      |
|----------------------|--------------|-------------|-------------|
| # passes per day     | 4.00         | 3.03        | 1.87        |
| Mean duration (s)    | 237.62       | 176.50      | 105.16      |
| Total duration (min) | <b>15.84</b> | <b>9.92</b> | <b>3.28</b> |

Table 9: Available connection time per day at lower orbits.

#### 4.1.3 Data budget calculation

For this calculation, information mentioned in section 2.3.4 and 4.1.1 is needed. The initial orbit for the Aalto-2 is not specified yet, that is why the data budget will be made for a 375 km height and a minimum elevation of 10°. Data used are:

- Average minutes per day: 21.49
- Bytes per frame: 6 + 256
- Bit rate: 9,600 bps

Considering those, it is possible to calculate the amount of data transmitted in a day at the beginning of the mission. Results are shown in Table 10.

| Field                         | 5,905.74 fr/day |                 |
|-------------------------------|-----------------|-----------------|
|                               | B/fr            | kB/day          |
| Overhead                      | 47              | 271.06          |
| Formation flight <sup>1</sup> | 20              | 0.02            |
| Telemetry                     | 60              | 346.04          |
| QB50 Science Data             | 43              | 247.99          |
| Remaining                     | 112             | 645.92          |
| Total                         | 262             | <b>1,511.04</b> |

Table 10: Data budget at the beginning of the mission.

It is important to know if there is a orbital height where is not possible to complain the requirement QB50-SYS-1.5.2 working at 9,600 bps. To know if it is possible to download 2 Mb per day even at the end of the mission, more simulations have been done at three different heights (300 km, 200 km and 100 km). The results are compared in Table 11.

---

<sup>1</sup>Formation flight data is sent only once per day.

| Field                         | 300 km, 4,353.04 fr/day |                 | 200 km, 2,726.15 fr/day |               | 100 km, 901.39 fr/day |               |
|-------------------------------|-------------------------|-----------------|-------------------------|---------------|-----------------------|---------------|
|                               | B/fr                    | kB/day          | B/fr                    | kB/day        | B/fr                  | kB/day        |
| Overhead                      | 47                      | 199.80          | 47                      | 125.13        | 47                    | 41.37         |
| Formation flight <sup>1</sup> | 20                      | 0.02            | 20                      | 0.02          | 20                    | 0.02          |
| Telemetry                     | 60                      | 255.06          | 60                      | 159.74        | 60                    | 52.82         |
| QB50 Data                     | 57.43                   | 244.14          | 91.70                   | 244.14        | 154.98                | 136.42        |
| Remaining                     | 97.57                   | 414.77          | 63.30                   | 168.51        | 0                     | 0             |
| Total                         | 262                     | <b>1,113.77</b> | 262                     | <b>697.51</b> | 262                   | <b>230.63</b> |

Table 11: Data budget at three different orbital heights.

The conclusion is that between 200 km and 100 km height there is not enough time for the communication between satellite and GS. Even reducing the housekeeping data to 0 kB per frame, it is possible to transmit only 1.1 Mb per day. To know the height where the Aalto-2 has to stop measuring with its own payload, the next equation has to be solved:

$$\frac{47 \cdot fr}{1024} + \frac{60 \cdot fr}{1024} + 244.14 = \frac{262 \cdot fr}{1024}, \quad (19)$$

where  $fr$  is the number of frames it will be possible to transmit in a day. The result of the equation is  $fr = 1,612.90$  frames per day, equivalent a 352.14 s/day. More simulations have been done with STK and the height where the communication lasts 352.14 seconds is at 149.5 km from the Earth's surface.

#### 4.1.4 Link budget calculation

Link budget have to be calculated for both uplink (UL) and downlink (DL) to assure that the communication is possible in both directions. As is explained in section 2.5.1, the *telecommunications link budget equation* shows the different important parameters for this calculation. As a reminder, the formula is as follows:

$$S/N_0 = P_T G_T (1/L_S) (1/L_A) (G_R/T_{sys}) (1/k). \quad (20)$$

It is possible to differentiate four terms in this equation:

- The EIRP of the transmitter:  $P_T G_T$ ;
- The total link losses:  $(1/L)$ ;
- The receiver's figure of merit:  $G_R/T_{sys}$ ;
- The inverse of the Boltzmann's constant:  $1/k$ ,

where  $L$  includes atmospheric losses, pointing losses, polarization losses and propagation losses calculated in the worst case, this is, with the satellite  $10^\circ$  over the horizon, where the maximum path length is 1,440 km. All of this terms depends on which link is being calculated, but the inverse of the Boltzmann's constant. This term will add 228.6 dB to the both links (UL and DL).

## Uplink

In this link, the transmitter (GS) produces a bit data rate of 1,200 bps with a frequency of 437.5 MHz. The output power is 30 W (14.8 dBW) but this power is affected by losses on the cables that have been used in its construction, connectors and losses inserted by the filter of the transmitter. The total losses have been approximated by 2.8 dB. Then, the electrical signal is converted to EM wave by the antenna characterized by a gain of 18.5 dBi. The total EIRP is, then

$$EIRP = 14.8 - 2.8 + 18.5 = 30.5 \text{ dBW}. \quad (21)$$

Then, as the signal travels, it is affected by the link losses, calculated in 150.7 dB. Finally, the signal is affected by the figure of merit of the Aalto-2 receiver which will be about -25.4 dB/K. This four main terms are shown in Table 12.

| EIRP     | Link losses | Figure of merit | $1/k$    | $S/N_0$ |
|----------|-------------|-----------------|----------|---------|
| 30.5 dBW | 150.7 dB    | -25.4 dB/K      | 228.6 dB | 83 dB   |

Table 12: Main terms in uplink budget.

To present the link budget in the two different ways ( $E_b/N_0$  and SNR), some modifications have to be made taken in care the bit rate  $R_b = 1,200$  bps and the receiver's band pass filter bandwidth  $B = 58$  kHz:

$$E_b/N_0 = 83 - 10 \cdot \log(R_b) = 52.2 \text{ dB}, \quad (22)$$

$$SNR = 83 - 10 \cdot \log(B) = 35.4 \text{ dB}. \quad (23)$$

Figure 16 shows in detail the gains and losses of the UL budget.

| Parameter:  | Value:           | Units: |
|---|------------------|--------|
| <b>Ground Station:</b>  |                  |        |
| Ground Station Transmitter Power Output:                                | 30,0             | watts  |
| In dBW:   | 14,8             | dBW    |
| In dBm:   | 44,8             | dBm    |
| Ground Stn. Total Transmission Line Losses:                             | 2,8              | dB     |
| Antenna Gain:   | 18,5             | dBi    |
| Ground Station EIRP:  | 30,5             | dBW    |
| <b>Uplink Path:</b>   |                  |        |
| Ground Station Antenna Pointing Loss:                                   | 0,5              | dB     |
| Gnd-to-S/C Antenna Polarization Losses:                                 | 0,2              | dB     |
| Path Loss:  | 148,4            | dB     |
| Atmospheric Losses:   | 1,1              | dB     |
| Ionospheric Losses:   | 0,4              | dB     |
| Rain Losses:  | 0,0              | dB     |
| Isotropic Signal Level at Spacecraft:                                   | -120,2           | dBW    |
| <b>Spacecraft (Eb/No Method):</b>                                       |                  |        |
| <b>Eb/No Method</b>   |                  |        |
| Spacecraft Antenna Pointing Loss:                                       | 0,0              | dB     |
| Spacecraft Antenna Gain:  | 1,0              | dBi    |
| Spacecraft Total Transmission Line Losses:                              | 0,8              | dB     |
| Spacecraft Effective Noise Temperature:                                 | 358              | K      |
| Spacecraft Figure of Merrit (G/T):                                      | -25,4            | dB/K   |
| S/C Signal-to-Noise Power Density (S/No):                               | 83,0             | dBHz   |
| System Desired Data Rate:   | 1200             | bps    |
| In dBHz:  | 30,8             | dBHz   |
| Command System Eb/No:   | 52,2             | dB     |
| Demodulation Method Selected:   | Non-Coherent FSK |        |
| Forward Error Correction Coding Used:                                   | None             |        |
| System Allowed or Specified Bit-Error-Rate:                             | 1,0E-05          |        |
| Demodulator Implementation Loss:  | 1,0              | dB     |
| Telemetry System Required Eb/No:  | 13,8             | dB     |
| Eb/No Threshold:  | 14,8             | dB     |
| <b>System Link Margin:</b>  | 37,4             | dB     |
| <b>Spacecraft Alternative Signal Analysis Method (SNR Computation):</b> |                  |        |
| <b>SNR Method</b>   |                  |        |
| Spacecraft Antenna Pointing Loss:                                       | 0,0              | dB     |
| Spacecraft Antenna Gain:  | 1,0              | dBi    |
| Spacecraft Total Transmission Line Losses:                              | 0,8              | dB     |
| Spacecraft Effective Noise Temperature:                                 | 358              | K      |
| Spacecraft Figure of Merrit (G/T):                                      | -25,4            | dB/K   |
| Signal Power at Spacecraft LNA Input:                                   | -120,0           | dBW    |
| Spacecraft Receiver Bandwidth:  | 58.000           | Hz     |
| Spacecraft Receiver Noise Power (Pn = kTB)                              | -155,4           | dBW    |
| Signal-to-Noise Power Ratio at G.S. Rcvr:                               | 35,4             | dB     |
| Analog or Digital System Required S/N:                                  | 14,4             | dB     |
| System Link Margin  | 21,0             | dB     |

Figure 16: Aalto-2 UL budget calculated with AMSAT-IARU Link Model.

## Downlink

In the downlink case, the Aalto-2 transmitter produces a bit data rate of 9,600 bps with a frequency of 437.45 MHz. The output power is 1 W (0 dBW) affected by the transmitter losses estimated in 1.2 dB. The antenna gain is 1 dBi and the EIRP has a value of

$$EIRP = 0 - 1.2 + 1 = -0.2 \text{ dBW}. \quad (24)$$

The link losses are the same than in the uplink case, 150.7 dB, because the 50 kHz shift between UL and DL is negligible when calculating the free space losses; and the figure of merit of the GS's receiver is -6 dB/K. This four main terms are shown in Table 13.

| EIRP     | Link losses | Figure of merit | $1/k$    | $S/N_0$ |
|----------|-------------|-----------------|----------|---------|
| -0.2 dBW | 150.7 dB    | -6 dB/K         | 228.6 dB | 71.7 dB |

Table 13: Main terms in downlink budget.

And the  $E_b/N_0$  and SNR are:

$$E_b/N_0 = 71.7 - 10 \cdot \log(R_b) = 31.9 \text{ dB}, \quad (25)$$

$$SNR = 71.7 - 10 \cdot \log(B) = 24.1 \text{ dB}, \quad (26)$$

where  $R_b = 9,600$  bps and  $B = 58$  kHz. Gains and losses are shown in detail in Fig 17.

## Link margins

Once the  $E_b/N_0$  of the two links is known, it is time to compare these results with the minimum  $E_b/N_0$  that the receivers need in order to understand what the transmitter sent. This minimum value is called  $E_b/N_0$  threshold and depends on the modulation used as well as the bit error rate (BER) desired. This parameter is the number of bit errors divided by the total number of transferred bits during a studied time interval and, for the Aalto-2, is set to  $1 \cdot 10^{-5}$  that means that, in average, there will be an error each 100,000 bits received. That fix the  $E_b/N_0$  threshold to 14.8 dB and the consequent link margins for both UL and DL:

$$UL \text{ link margin} = 52.2 \text{ dB} - 14.8 \text{ dB} = 37.4 \text{ dB}, \quad (27)$$

$$DL \text{ link margin} = 31.9 \text{ dB} - 14.8 \text{ dB} = 17.1 \text{ dB}. \quad (28)$$

As can be seen, there is a 20.3 dB difference between the two margins. This is mostly due to the higher output power of the GS transmitter which is not affected by the available power that suffers the satellite. Despite this fact, both margins are high enough to ensure a successful communication. In the Annex A there is the detailed link budget.

| Parameter:  | Value:           | Units:    |
|---|------------------|-----------|
| <b>Spacecraft:</b>  |                  |           |
| Spacecraft Transmitter Power Output:  | 1,0 watts        |           |
| In dBW:   | 0,0              | dBW       |
| In dBm:   | 30,0             | dBm       |
| Spacecraft Total Transmission Line Losses:                                  | 1,2 dB           |           |
| Spacecraft Antenna Gain:  | 1,0 dBi          |           |
| Spacecraft EIRP:  | -0,2             | dBW       |
| <b>Downlink Path:</b>   |                  |           |
| Spacecraft Antenna Pointing Loss:   | 0,0 dB           |           |
| S/C-to-Ground Antenna Polarization Loss:                                    | 0,2 dB           |           |
| Path Loss:  | 148,4 dB         |           |
| Atmospheric Loss:   | 1,1 dB           |           |
| Ionospheric Loss:   | 0,4 dB           |           |
| Rain Loss:  | 0,0 dB           |           |
| Isotropic Signal Level at Ground Station:                                   | -150,4           | dBW       |
| <b>Ground Station (EbNo Method):</b>  |                  |           |
| <b>----- Eb/No Method -----</b>   |                  |           |
| Ground Station Antenna Pointing Loss:                                       | 0,5 dB           |           |
| Ground Station Antenna Gain:  | 18,5 dBi         |           |
| Ground Station Total Transmission Line Losses:                              | 0,9 dB           |           |
| Ground Station Effective Noise Temperature:                                 | 229 K            |           |
| Ground Station Figure of Merrit (G/T):                                      | -6,0 dB/K        |           |
| G.S. Signal-to-Noise Power Density (S/No):                                  | 71,7             | dBHz      |
| System Desired Data Rate:   | 9600             | bps       |
| In dBHz:  | 39,8             | dBHz      |
| Telemetry System Eb/No for the Downlink:                                    | 31,9             | dB        |
| Demodulation Method Selected:   | Non-Coherent FSK |           |
| Forward Error Correction Coding Used:                                       | None             |           |
| System Allowed or Specified Bit-Error-Rate:                                 | 1,0E-05          |           |
| Demodulator Implementation Loss:  | 1                | dB        |
| Telemetry System Required Eb/No:  | 13,8             | dB        |
| Eb/No Threshold:  | 14,8             | dB        |
| <b>System Link Margin:</b>  | <b>17,1</b>      | <b>dB</b> |
| <b>Ground Station Alternative Signal Analysis Method (SNR Computation):</b> |                  |           |
| <b>----- SNR Method -----</b>   |                  |           |
| Ground Station Antenna Pointing Loss:                                       | 0,5 dB           |           |
| Ground Station Antenna Gain:  | 18,5 dBi         |           |
| Ground Station Total Transmission Line Losses:                              | 0,9 dB           |           |
| Ground Station Effective Noise Temperature:                                 | 229 K            |           |
| Ground Station Figure of Merrit (G/T):                                      | -6,0 dB/K        |           |
| Signal Power at Ground Station LNA Input:                                   | -133,3           | dBW       |
| Ground Station Receiver Bandwidth (B):                                      | 58.000           | Hz        |
| G.S. Receiver Noise Power (Pn = KTB)  | -157,4           | dBW       |
| Signal-to-Noise Power Ratio at G.S. Rcvr:                                   | 24,1             | dB        |
| Analog or Digital System Required S/N:                                      | 16,6             | dB        |
| System Link Margin  | 7,5              | dB        |

Figure 17: Aalto-2 DL budget calculated with AMSAT-IARU Link Model.

## 4.2 Aalto-2 antenna subsystem design

Communication between satellite and GS is performed by using the antennas. In this case, the frequency that is going to be used is located in the UHF band, i.e. in the megahertz band which requires a relatively big antennas in relation with the size of a CubeSat. Moreover, the goal of the CubeSat standard is to reduce the budget that implies to put in orbit a satellite, so it makes sense to figure out the way for the satellite to fill in the minimum space possible before to be released.

This way, the space that the Launch Vehicle (LV) has, would be exploited at maximum, making possible the launch of several CubeSats with the same rocket, sharing the cost of the launch. Thus, the goal of the ADS design is to develop the antennas of the satellite in a way that, before to be deployed the size of the satellite not to overpass the maximum size specified for a CubeSat, meanwhile it is assured a desired behaviour when they are deployed.

In the following sections, the ADS requirements will be presented as well as the study was carried out with the aim of designing the antennas with a suitable parameters for their future use, and how they communicate with the transmitter/receiver.

### 4.2.1 3D-representation of the satellite

In order to find the best configuration for the antennas, it has been used CST Studio, the same software used in the ADS design of the Aalto-1 satellite. The body of the satellite has been modelled as a simple aluminium block being  $+Z$  the direction of flight. This will reduce the calculation's load and thus, the simulation time. Supports for solar panels have been added to the body, using the same material. These panels, although adds complexity to the simulation, might affect the behaviour of the antennas, so it was decided to include them in the simulations. Its design was obtained from the project documentation and is shown in Fig. 18.

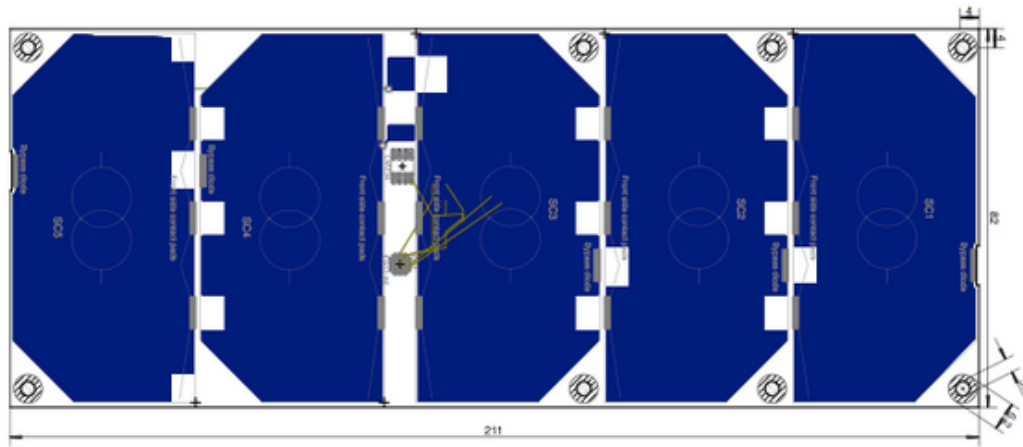


Figure 18: Mechanical drawing of the solar panel. Dimensions in millimeters [40].

Antennas have to be added to this 3D-model and they are modelled as a Perfect Electric Conductor (PEC). The material that isolates the antennas and avoids any contact with the satellite body will be polyamide, a semi-crystalline polymer with a very good mechanical properties. The Aalto-2 3D-drawing is shown in Fig. 19.

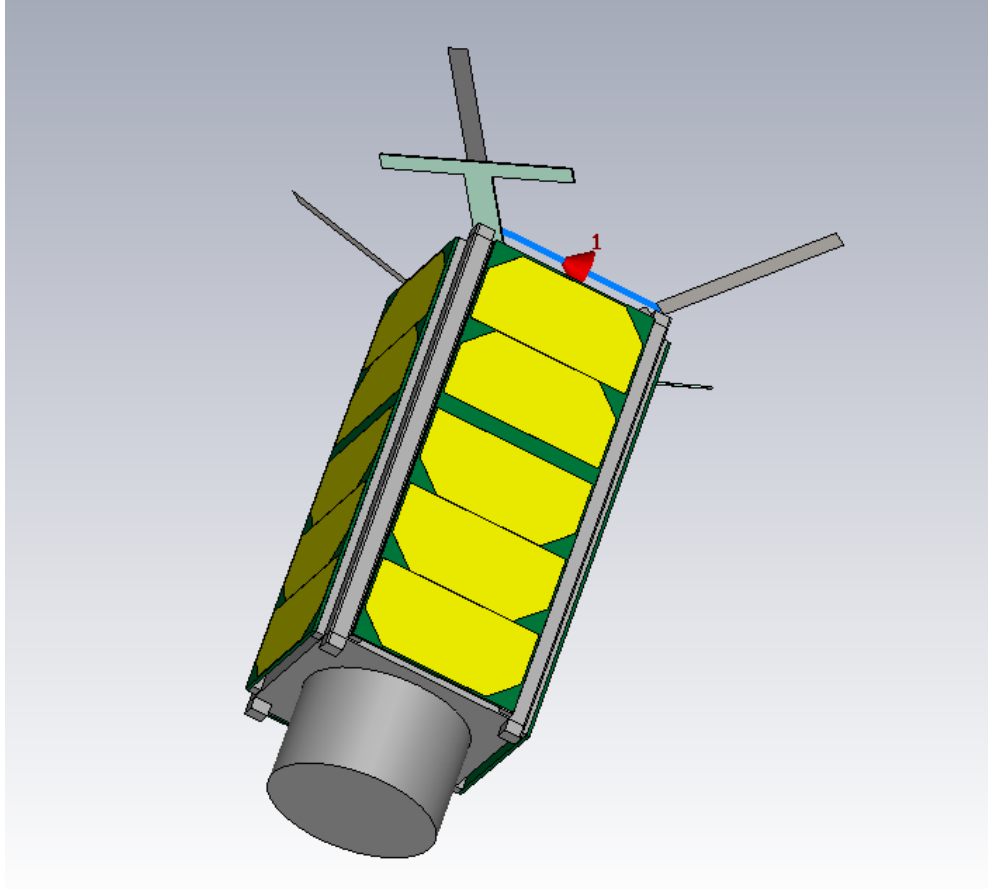


Figure 19: 3D-representation of the Aalto-2 satellite.

#### 4.2.2 Antenna design

In order to save mass for other subsystems, the ADS mechanism should be as light as possible. It should also be taken into account the volume occupied, because it could occupy the space dedicated for other systems. For this reason, different antenna designs have been considered for the ADS. All of them share a similar performance: the antennas may not protrude the maximum sizes before and during the launch and are released in a timely manner.

A widespread technique for CubeSats is to use flexible antennas and nylon fishing line in order to keep the antennas folded. Once out the P-POD, “all deployables such as booms, antennas, and solar panels shall wait to deploy a minimum of 30 minutes after the CubeSat’s deployment switch(es) are activated from P-POD ejection” [13]. This process can be controlled by the OBC but, given the good results

that the Aalto-1 ADS tests have shown, it is very likely to use the same system: one independent Printed Circuit Board (PCB) whose main component is a timer.

An important requirement when finding the best way to fold the antennas is the fact that the antenna will be used as stabilizers. This is because the attitude of the satellite will be affected by the atmosphere while descending during its lifetime until 90 km high. Thus, the antennas will help the ADCS to maintain the attitude and this is possible only if they face their broad side towards the direction of flight as is shown in the previous Fig. 19.

That is why it was decided to use two half-wave dipoles bended  $120^\circ$  (an angle calculated by the mechanical team in order to use antennas as stabilizers against the gasses of the atmosphere). The first idea was to attach the antennas in the end plate folding the antennas around the satellite in the direction of flight. This technique has been used for some CubeSats like the KySat-1 developed in Kentucky (USA) which is shown in Fig. 20.

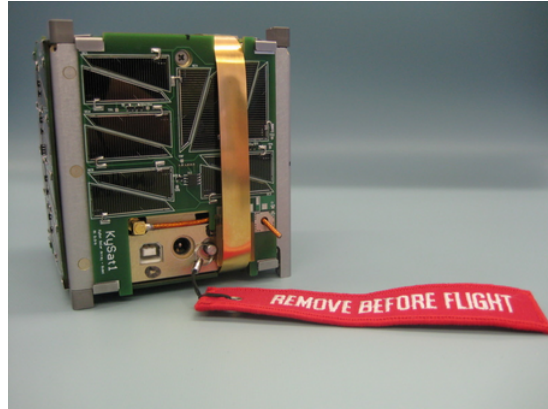


Figure 20: KySat-1 with the antennas folded over the solar panels [41].

This idea was rejected by the team due to the risk of damaging the solar panels provoked by the vibration that the satellite suffers during the launch. The next solution came due to an ambiguity in the QB50 documentation where there was the possibility of having a second extended volume at the back of the satellite. That placement for the antenna could have been a good solution for the problem, but finally, after contact the QB50 consortium, it was impossible to put the antennas outside the body of the satellite. So, if the antennas could not be folded outside the satellite, they have to be folded inside it with the disadvantage of having less space for other payloads or subsystems.

It was decided to use a cross-shape box at the back of the satellite where the antennas will be folded as well as two symmetric doors to help in the stabilization of the satellite. These doors have the shape of a split cross through one of its symmetry planes as can be seen in the following figure. The antennas were simulated with the

configuration visible in Figure 19 but with two different ways to connect the arms of the dipoles. They are shown in Fig. 21.

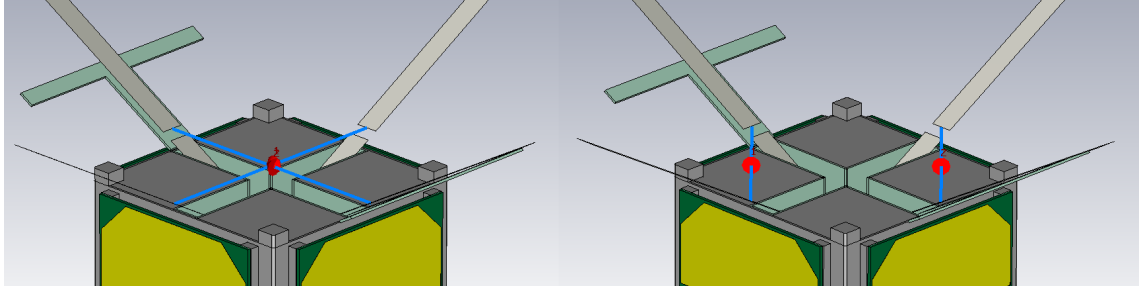


Figure 21: Two possible connections for the arms of the dipoles.

Both configurations were simulated with a phase shift of  $0^\circ, 90^\circ, 180^\circ$  and  $270^\circ$  between the two signals that feed the dipoles. Between the 8 results obtained, in Figure 22 is presented the best radiation pattern (achieved with  $0^\circ$  of phase shift) for each configuration when  $\theta = 60^\circ$ , i.e. when the GS see the satellite  $60^\circ$  over the horizon. The signal power is presented in dB for any value of  $\phi$ .

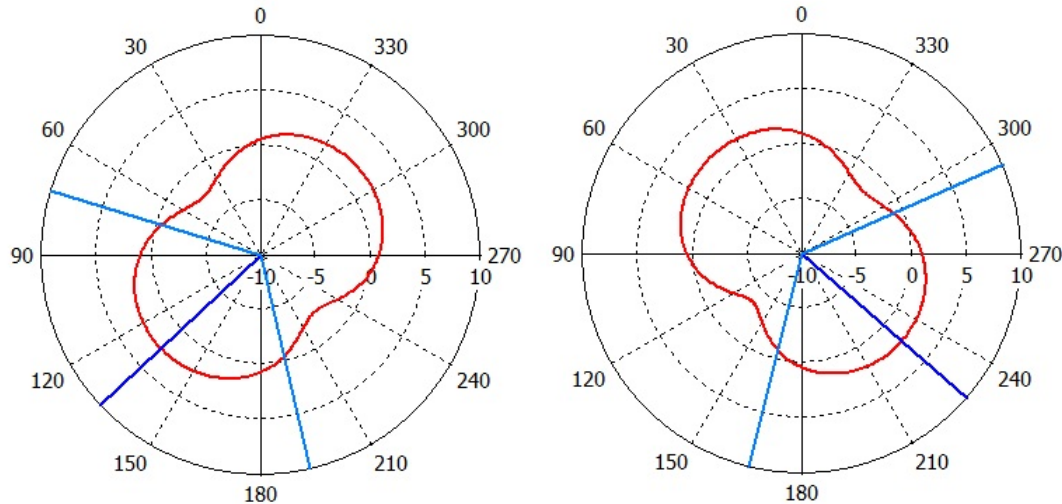


Figure 22: Radiation pattern for the 2 connect configurations.

It is important to notice that the ideal radiation pattern would be omnidirectional as the satellite might tumble during the communication session. Since this antenna behaviour can not be achieved, is preferable to have the maximum of radiation in the nadir and a big beamwidth. In the last figure, it is easy to see that the maximum of radiation is shifted from the desirable direction, so the ADS and the antennas were turned  $45^\circ$  for the following simulations. Again, the two possible ways to connect the arms of the dipoles and the four phase shifts were simulated. The results were similar to the previous ones but with the maximum of radiation pointing at nadir.

### 4.2.3 Antenna parameters

Finally, the connection shown in Figure 23 and a  $0^\circ$  phase shift was selected as the final antenna design. Optimization of the design was performed varying the length of the antennas in order to have as low return loss (characterized by the parameter  $S11$ ) as possible. The length of the arms that gave the best antenna parameters working at 437.5 MHz was 96.65 mm and the resulting parameters are in the following list:

- Antenna configuration: Two  $120^\circ$  bended dipoles
- Arm length: 96.65 mm
- Return loss: -31.5 dB
- Impedance:  $Z_A = 52.62 - i0.67 \Omega$  ( $Z_{Optimum} = 50 \Omega$ )
- Antenna efficiency: -0.04351 dB,  $\mu_l = 99\%$
- Main gain at nadir: 1 dB
- Polarization: linear
- Gap with the antenna extender: 4 mm
- Distance to satellite end plate: 10 mm

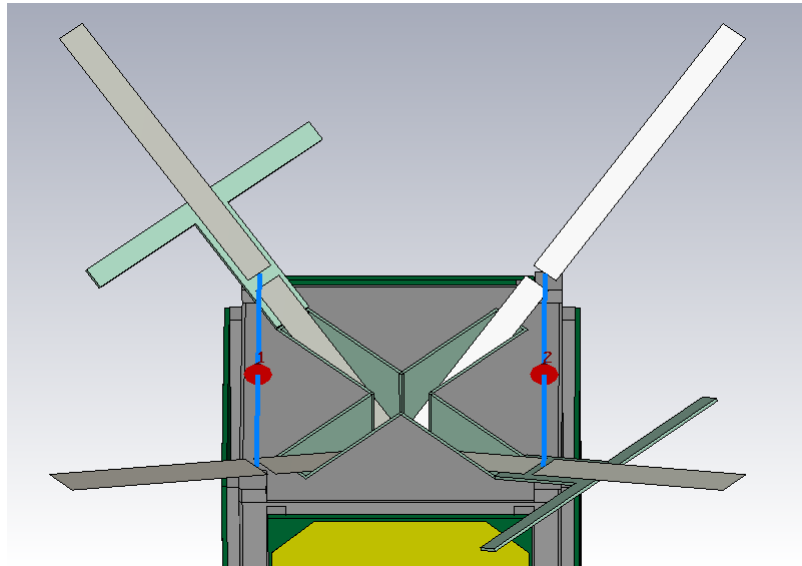


Figure 23: Final connection for the Aalto-2 antennas.

In order to know how the radiated power change when the satellite passes through the sky, in Figure 24 and Figure 25 are presented some 2D-diagrams for different values of  $\theta$  as well as the  $S11$  parameter graph, but for more detail see Annex C, where are draws of the radiation pattern every  $10^\circ$ .

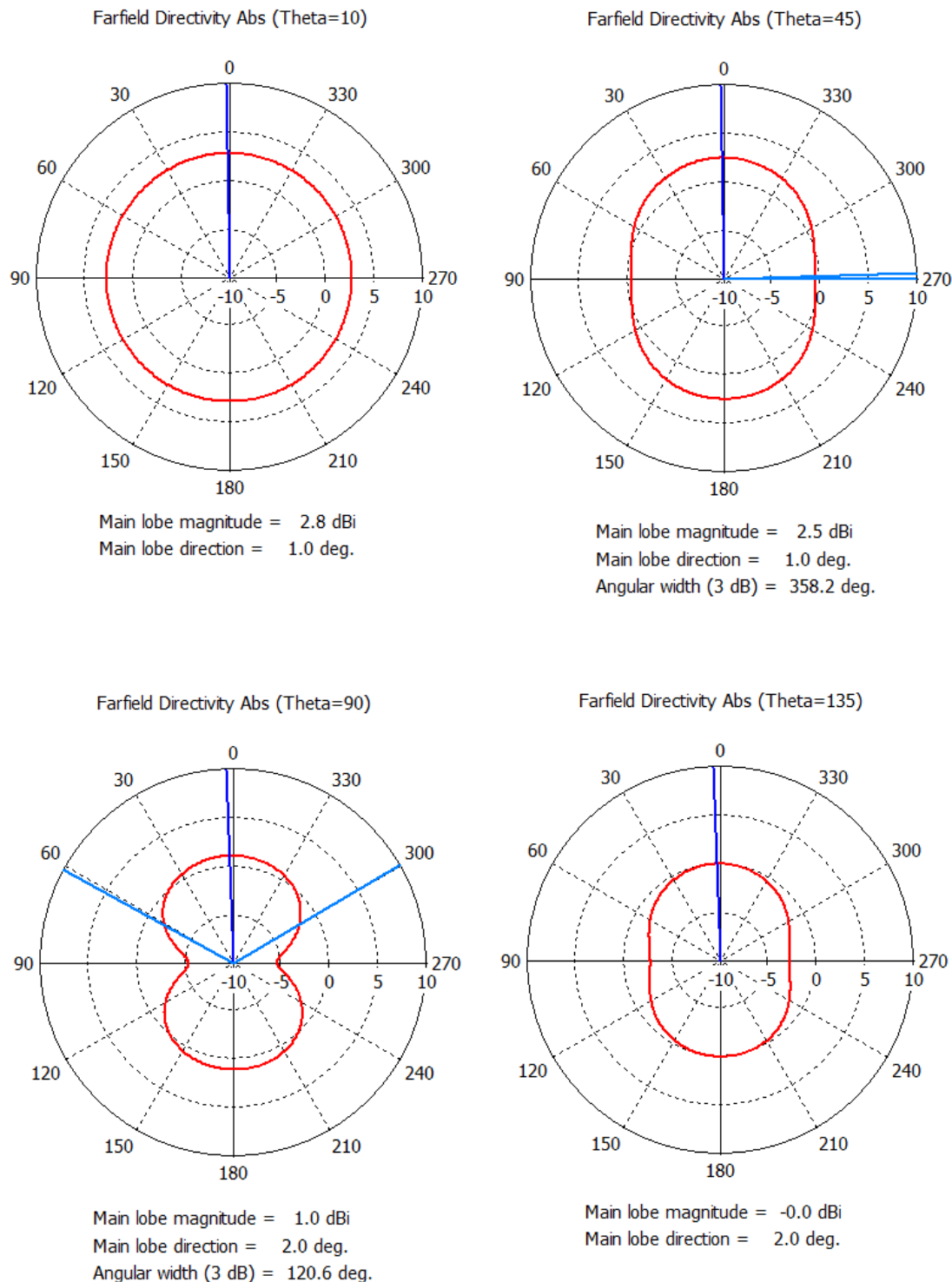


Figure 24: 2D radiation pattern for  $\theta = 10^\circ, 45^\circ, 90^\circ$  and  $135^\circ$ .

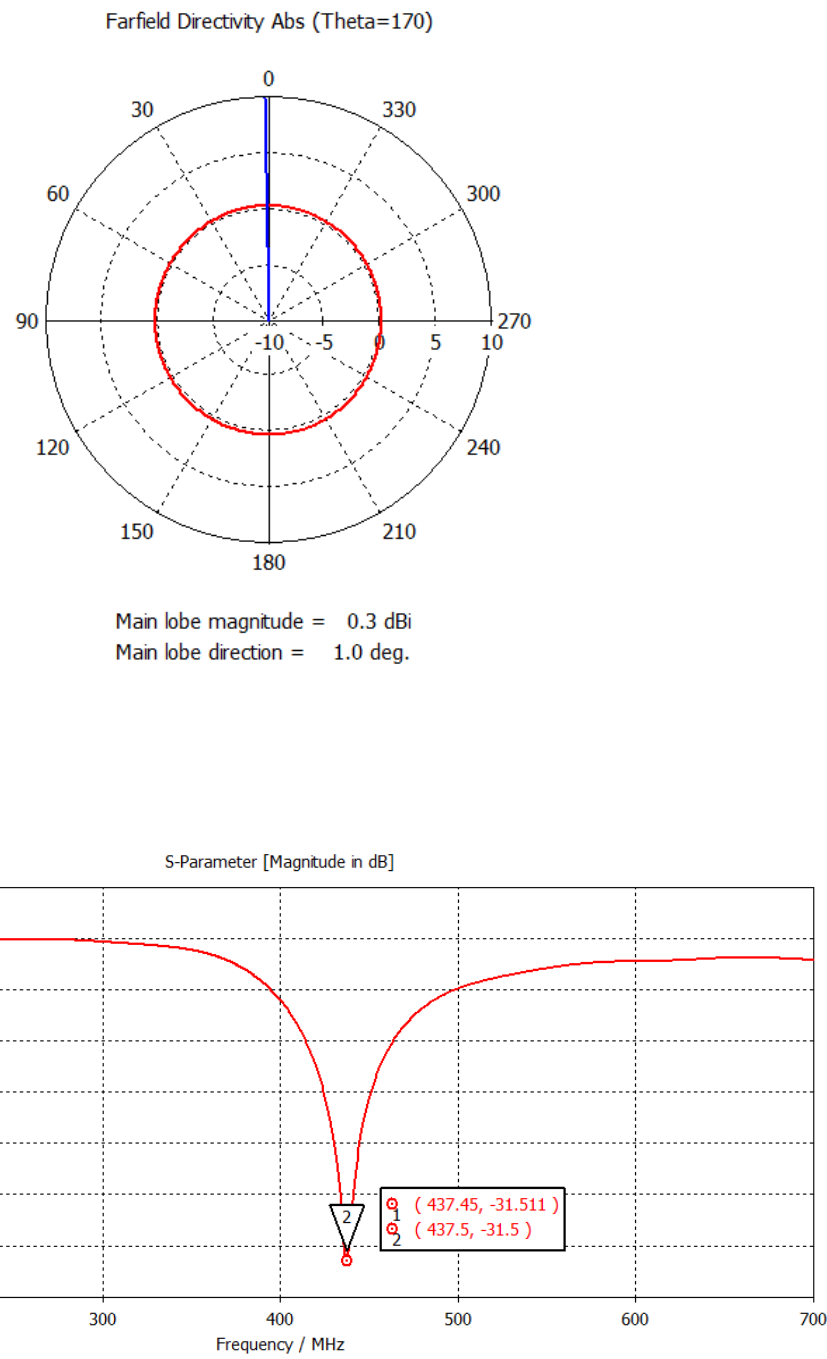


Figure 25: 2D radiation pattern for  $\theta = 170^\circ$  and  $S11$  graph.

#### 4.2.4 Antenna Deployment System design

The holder for the antennas is a cross-shaped box merged with the top plate of the satellite. This piece of the ADS is shown in Figure 26. For more detail, see technical drawing of the antenna holder in Annex B. The main part of the ADS is the timer circuit, explained below.

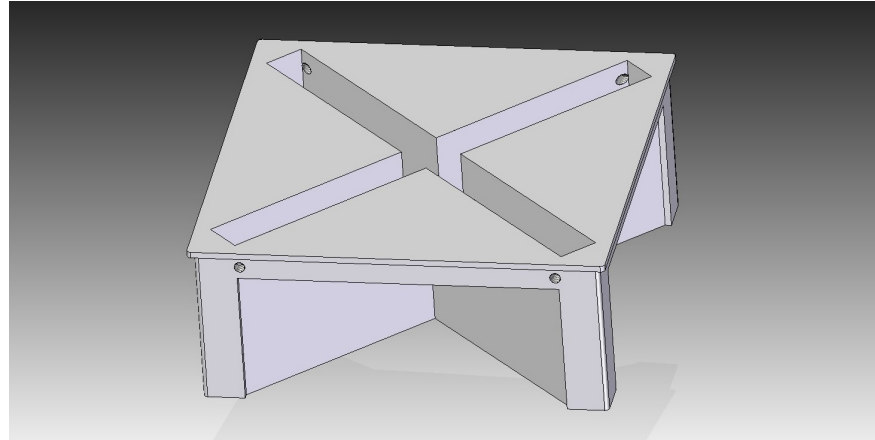


Figure 26: Antenna holder.

#### Timer Circuit

As already explained, the OBC will not control the deployment of the antennas, instead a separate timer circuit board will perform the task. To take full advantage of the knowledge gained through the design of the Aalto-1 [42], it was decided to use the same timer chip as the main component of the timer circuit. This chip, CD4060BM, is developed by Texas Instruments and its Small Outline Integrated Circuit (SOIC) is shown in Fig. 27.



Figure 27: Texas Instruments' circuit timer CD4060BM.

Chip features include a wide operating voltage range from -0.5 to 20 V and a wide operating temperature range from  $-55^{\circ}\text{C}$  to  $+125^{\circ}\text{C}$  [43]. CD4060BM is a 14-stage ripple carry binary counter. The counters are advanced one count on the negative transition of each clock pulse given by an external RC-circuit. The counters are reset to the zero state by a logical '1' at the reset input independent of clock [43]. The schematic and connection diagrams are shown in Figure 28 and Figure 29.

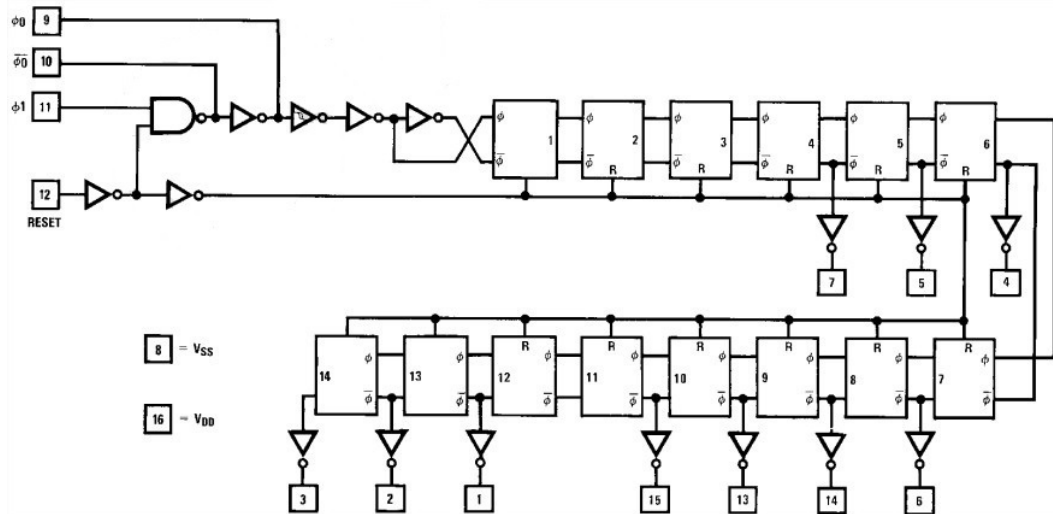


Figure 28: CD4060BM Schematic diagram showing the logical structure of the component [43].

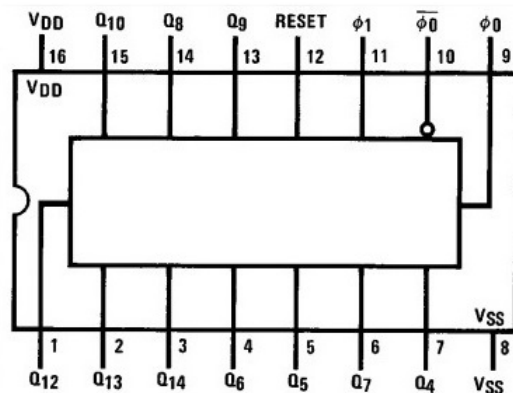


Figure 29: CD4060BM Connection diagram showing the pin assignments [43].

To manage the time delay, two factors must be taken into account: the frequency of the oscillator and which output stage is chosen. The oscillation frequency is calculated using the formula:

$$f = \frac{1}{2.2R_1C}, \quad (29)$$

where  $R_1$  and  $C$  are the electric components which control the oscillation frequency shown in Figure 30. The total delay is calculated by the formula:

$$t = \frac{2^{n-1}}{f}, \quad (30)$$

where  $n$  is the selected Q output number. Since the needed time delay is 30 minutes, it is possible to assign the following parameters:

- $R_1 = 1 \text{ M}\Omega$
- $C = 220 \text{ nF}$
- $n = 13$

This way, the frequency would be 2.066 Hz and the total delay 33 min.

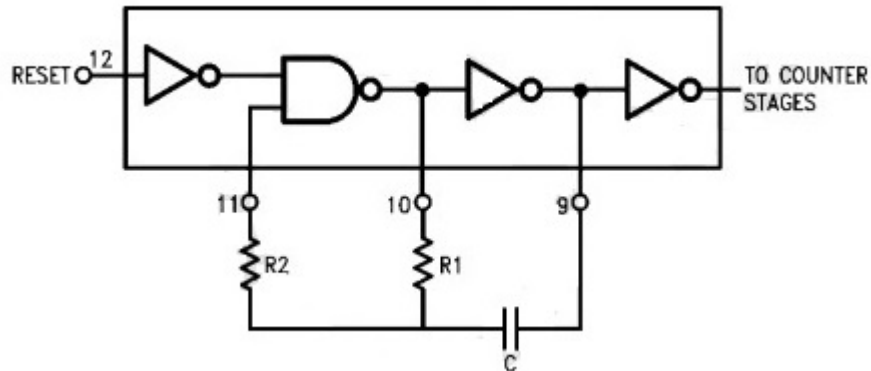


Figure 30: CD4060BM RC Oscillator diagram [43].

A very important technique is the use of redundancy in the components to assure the deployment of the antenna. That is why is advisable the use of at least two heating resistors to burn the nylon fishing line that will maintain the doors closed.

## 5 Future work

Due to time constraints, it was not possible to develop a complete antenna system in the framework of this work but the deployment mechanism has to be tested tens of times before building the ADS that will be launched to space. The future work to be carried out by Aalto-2 team before these tests, is presented here.

### 5.1 Prototyping

The first step will be to build a prototype. The antenna holder can be printed in a 3D-printer and the antennas can be made from a common measuring tape. Each antenna assembly, shown in Figure 31, consists of the antenna extender, two antenna connectors and two dipole arms. Antenna connectors are used to connect antenna extender to the antennas and are made from Polyoxymethylene plastic [42].



Figure 31: Antenna assembly [42].

### 5.2 ADS testing and Radiation pattern measurements

Once the prototype is build, antenna deployment tests have to be performed in order to detect possible mistakes in the deployment mechanism (timer circuit, heating resistors, antenna doors, etc.). It is also important to measure the radiation pattern simulated with CST Studio once the prototype is build. This measurements are performed in an anechoic chamber which is a chamber completely isolated from signals that can interfere the antennas. Figure 32 shows the radiation pattern measurements done for the CubeSat CubeCat-1, from the Polytechnic University of Catalonia.



Figure 32: Radiation pattern measurement in an anechoic chamber [44].

## 6 Conclusions

In this work, a complete radio link solution was designed for Aalto-2 nanosatellite. The work included antenna design, link budget and data budget calculations and theoretical introduction to satellite communication subject. Presented communication design complies all the requirement set for the Aalto-2 mission presented in section 2.2.2.

The most difficult was to meet the data budget requirement, set by QB50 project science payload. As it was shown, the required amount of data per day is not difficult to achieve at the beginning of the mission but it can not be achieved under 149.5 km over the Earth's surface. At the end of the mission, it is possible to transmit only half of data requested. Compliance of this requirement does not depend on the satellite, but the orbit in which it is released. That's why it has no solution.

The presented link budget for the Aalto-2 has a high enough link margin to withstand additional losses in the troposphere caused by variable meteorological conditions. The uplink is usually not the most difficult in satellite communication as the ground station transmission power can be adjusted. Instead, due to the limitations in power that the satellite has, the downlink margin is very important. In this case, the result has been a SNR downlink margin of 7.5 dB.

The antenna design presented here has suitable, almost omnidirectional, radiation pattern and additionally the antennas can be used as additional stabilizers for the satellite attitude. Results obtained are a maximum of radiation in the nadir direction with a value of 2 dB with a beamwidth of 120°. Optimization of the antenna varying the antenna length and the gap between the antenna extenders and the arms of the dipoles, has resulted in an antenna matching of -31.5 dB.

To help Aalto-2 team on the future work, a preliminary design of the Antenna Deployment System has also been presented. The main part is the design of the antenna holder and the doors, which have the goal to maintain the antennas coiled inside the body of the satellite in order to satisfy the CubeSat standard.

Finally, it have been presented the two next steps that the Aalto-2 team has to carry out in order to verify the antenna behaviour simulated and finish the ADS design.

## References

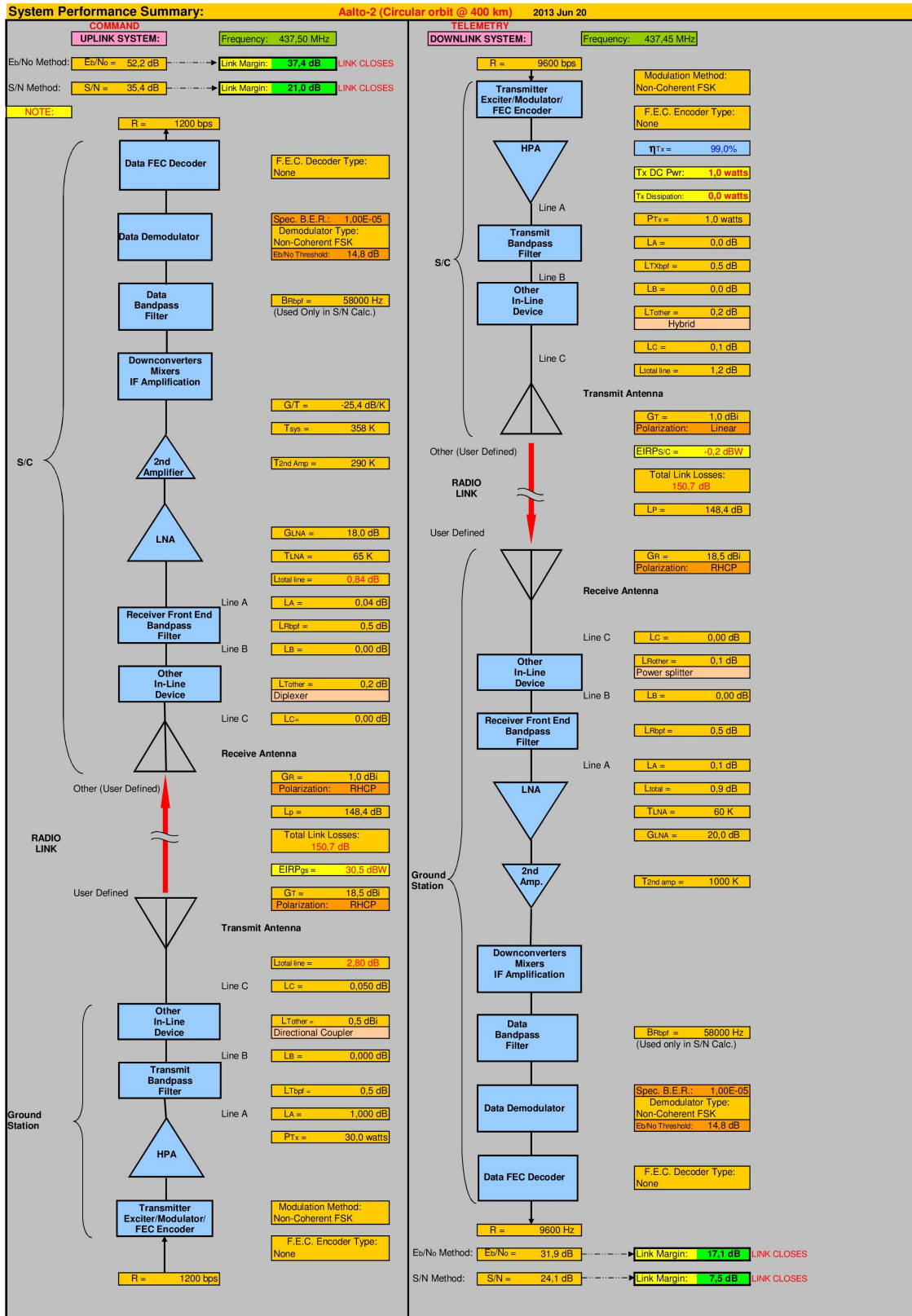
- [1] Goleniewski, L. and Jarrett, K. W. *Telecommunications Essentials, Second Edition: The Complete Global Source*, 2nd edition, Addison-Wesley Professional, 2006.
- [2] Bilsing, A. *OSCAR-1 Launched 50 Years Ago*, ARRL's Space Communication. Accessed Mar. 22, 2013. Available from: <http://www.arrl.org/files/file/Technology/Bilsing.pdf>.
- [3] Long, K. *Space Travel*, The British Interplanetary Society. Accessed Mar. 22, 2013. Available from: <http://www.bis-space.com/inf/space-travel>.
- [4] Fortescue, P., Swinerd, G. and Stark, J. *Spacecraft Systems Engineering*, 4th edition, Wiley, 2011.
- [5] *UoSat 1, 2*, Gunter's Space, 2013. Accessed Mar. 25, 2013. Available from: [http://space.skyrocket.de/doc\\_sdat/uosat-1.htm](http://space.skyrocket.de/doc_sdat/uosat-1.htm).
- [6] *UoSAT-1: The Mission*, Surrey Satellite Technology LTD. Accessed Mar. 22, 2013. Available from: <http://www.sstl.co.uk/Missions/UoSAT-1--Launched-1981/UoSAT-1/UoSAT-1--The-Mission>.
- [7] *UoSAT-2: The Mission*, Surrey Satellite Technology LTD. Accessed Mar. 22, 2013. Available from: <http://www.sstl.co.uk/Missions/UoSAT-2--Launched-1984/UoSAT-2/UoSAT-2--The-Mission>.
- [8] VEGA maiden flight VV01, ESA, 2012. Accessed Jun. 12, 2013. Available from: [http://www.esa.int/Our\\_Activities/Launchers/Launch\\_vehicles/Vega3/Cubesats](http://www.esa.int/Our_Activities/Launchers/Launch_vehicles/Vega3/Cubesats).
- [9] Kestila, A. et al. *Aalto-1 nanosatellite technical description and mission objectives*, Aalto University, 2013. Available from: <http://www.geosci-instrum-method-data-syst.net/2/121/2013/gi-2-121-2013.pdf>.
- [10] *QB50 project description*, QB50 Project. Accessed Apr. 9, 2013. Available from: <http://qb50.eu/index.php/project-description>.
- [11] Evans, B. G. *Satellite Communication Systems*, 3rd edition, The Institution of Engineering and Technology, 1999.
- [12] *Satellite Subsystems*, InetDaemon.Com, 2012. Accessed Mar. 27, 2013. Available from: [http://www.inetdaemon.com/tutorials/satellite/satellite\\_subsystems.shtml](http://www.inetdaemon.com/tutorials/satellite/satellite_subsystems.shtml).
- [13] *CubeSat Design Specifications Rev12*, The CubeSat Program, 2009. Accessed May 15, 2013. Available from: <http://www.cubesat.org/index.php/documents/developers>.

- [14] Moreno, O. A. *CubeSat - Introducción*, The Robotics Institute of Yucatán (TRIY), 2009. Accessed May 15, 2013. Available from: [http://www.triy.org/ESP/CubeSat\\_Intro.htm](http://www.triy.org/ESP/CubeSat_Intro.htm).
- [15] Nugent, R. et al. *The CubeSat: The Picosatellite Standard for Research and Education*, California Polytechnic State University, 2008. Available from: [http://cubesat.org/images/More\\_Papers/cps2008.pdf](http://cubesat.org/images/More_Papers/cps2008.pdf).
- [16] Fitzpatrick, R. *An Introduction to Celestial Mechanics*, University of Texas at Austin, 2013. Available from: <http://farside.ph.utexas.edu/teaching/celestial/Celestial.pdf>.
- [17] Morbidelli, A. *Modern celestial mechanics: aspects of solar system dynamics*, Taylor & Francis, 2002.
- [18] Hernandez, M. *Satellite Orbital Motion*, Polytechnic University of Catalonia (UPC), 1998. Accessed Jun. 13, 2013. Available from: <http://gage14.upc.es/manuel/tdgps/node11.html>.
- [19] Nave, R. *Ellipses and Elliptic Orbits*. Accessed Apr. 4, 2013. Available from: <http://hyperphysics.phy-astr.gsu.edu/hbase/math/ellipse.html>.
- [20] *How Satellite Works*, VT iDirect. Accessed Apr. 4, 2013. Available from: <http://www.idirect.net/Company/Resource-Center/Satellite-Basics/How-Satellite-Works.aspx>.
- [21] *Definition of Two-line Element Set Coordinate System*, NASA, 2011. Accessed Jun. 13, 2013. Available from: [http://spaceflight.nasa.gov/realdata/sightings/SSapplications/Post/JavaSSOP/SSOP\\_Help/tle\\_def.html](http://spaceflight.nasa.gov/realdata/sightings/SSapplications/Post/JavaSSOP/SSOP_Help/tle_def.html).
- [22] Praks, J. *Aalto-1 Project Management Plan*, A1-M-PL-01, version 1, Aalto-1 project documentation. Aalto University, 24 Aug 2011.
- [23] Praks, J., Kestilä, A. and Hallikainen, M. *Aalto-2 Project Management Plan*, A2-M-PL-01, version 5, Aalto-2 project documentation. Aalto University, 24 Mar 2013.
- [24] *QB50 CubeSat Requirements, Recommendations and Interface Control Document*, issue 3, QB50 Project, 2013. Accessed May 15, 2013. Available from: <http://www.qb50.eu/index.php/requirements-and-reviews>.
- [25] Ippolito, L. J. and Nostrand-Reinold, V. *Radiowave Propagation in Satellite Communications*, Springer, 1986.
- [26] Jordan, E. C. and Balmain, K. G. *Electromagnetic waves and radiating systems*, 2nd edition, Prentice-Hall, Inc., 1968.

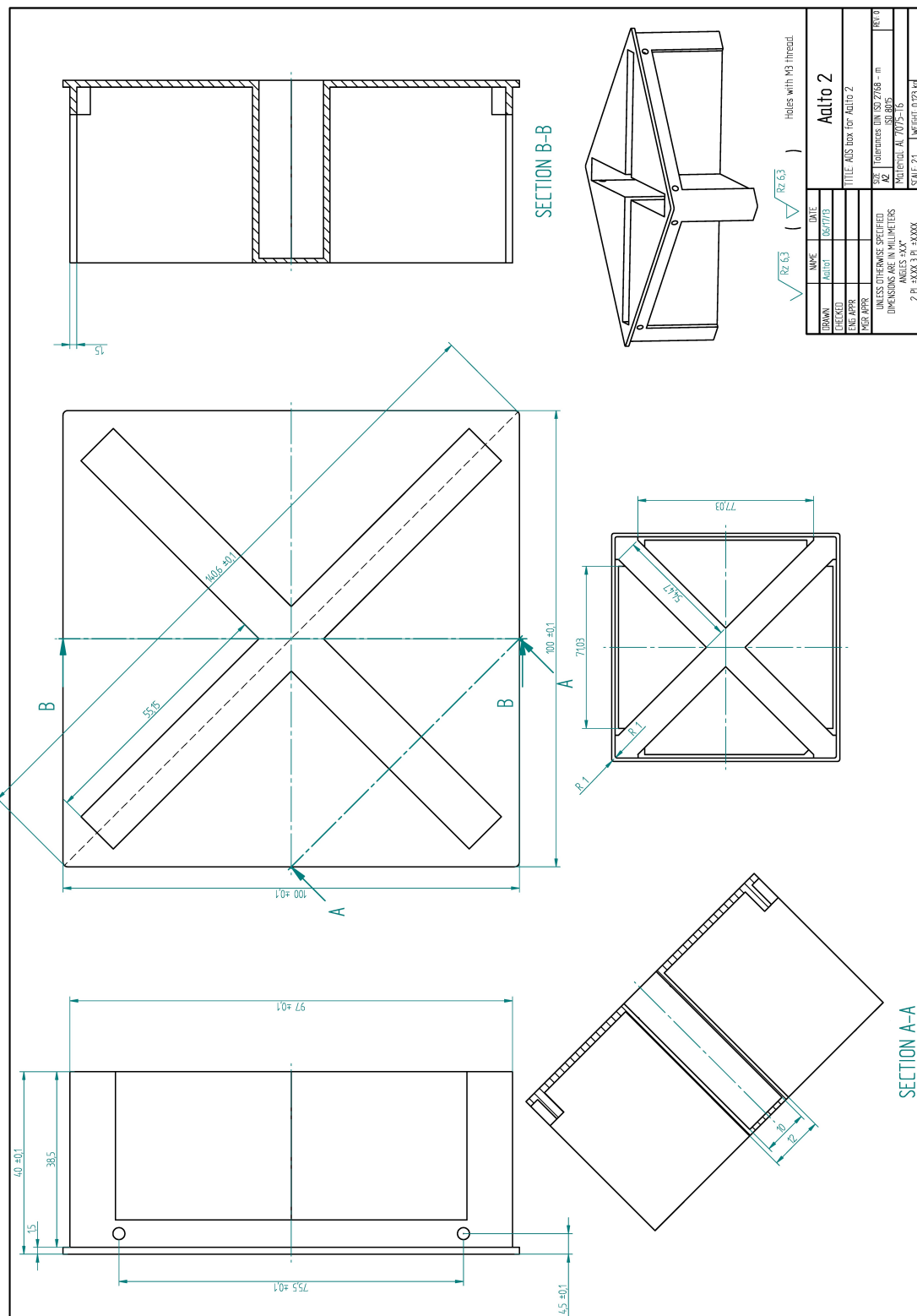
- [27] *The electromagnetic spectrum*. Accessed Apr. 30, 2013. Available from: <https://audioboo.fm/boos/151782-the-electromagnetic-spectrum>.
- [28] *ITU Recommendation V.431-7: Nomenclature of the frequency and wavelength bands used in telecommunications*, ITU, 2000. Available from: [http://www.itu.int/dms\\_pubrec/itu-r/rec/v/R-REC-V.431-7-200005-I!!PDF-E.pdf](http://www.itu.int/dms_pubrec/itu-r/rec/v/R-REC-V.431-7-200005-I!!PDF-E.pdf).
- [29] Signell, P. *Electromagnetic waves from maxwell's equations*, Michigan State University, 2001. Available from: [http://www.physnet.org/modules/pdf\\_modules/m210.pdf](http://www.physnet.org/modules/pdf_modules/m210.pdf).
- [30] Parry-Hill, M. J., Sutter, R. T. and Davidson, M. W. *Basic Electromagnetic Wave Properties*, National High Magnetic Field Laboratory, 2006. Accessed May 3, 2013. Available from: <http://micro.magnet.fsu.edu/primer/java/wavebasics>.
- [31] Hall, M. *Effects of the Troposphere on Radio Communications*, Institution of Engineering and Technology, 1980.
- [32] B. W. Marsden, *Communication network protocols*, 2nd edition, Blenheim Online Pubns, 1986.
- [33] Beech, W. A., Nielsen, D. E. and Taylor, J. *AX.25 Link Access Protocol for Amateur Packet Radio*, version 2.2, 1998. Available from: <http://www.tapr.org/pdf/AX25.2.2.pdf>.
- [34] Partridge, C. and Hinden, R. *Version 2 of the Reliable Data Protocol*, 1990. Accessed Feb. 20, 2013. Available from: <http://tools.ietf.org/html/rfc1151>.
- [35] Rius, J. M. et al. *Antenas*, 2nd edition, Edicions UPC, 2002.
- [36] *Polarization maintaining*, Fibrepulse. Accessed May 20, 2013. Available from: <http://www.fibrepulse.com/html/polar1.html>.
- [37] Barringer, M. H. and Springer, K. D. *Radiowave propagation*, 2013. Available from: [http://www.maisonsthenezay.fr/Maintenance\\_HF/NAB\\_files/2-01.pdf](http://www.maisonsthenezay.fr/Maintenance_HF/NAB_files/2-01.pdf).
- [38] Satellite Tool Kit, Analytical Graphics, Inc. 2013. Accessed May 8, 2013. Available from: <http://www.agi.com/products>.
- [39] CST website, Computer Simulation Technology AG., 2013. Accessed May 8, 2013. Available from: <http://www.cst.com>.
- [40] Hemmo, J. *Aalto-2 Electrical Power System Design*, A2-EPS-DD-01, version 1, Aalto-2 project documentation. Aalto University, 8 Mar 2013.

- [41] *KySat-1 Image Gallery*, Space Systems Laboratory. Accessed Jun 11, 2013. Available from: <http://ssl.engineering.uky.edu/missions/orbital/kysat1/images/>.
- [42] Lankinen, M. *Aalto-1 Design of Antenna Deployment System*, A1-MEC-DD-03, version 1, Aalto-1 project documentation. Aalto University, 28 May 2013.
- [43] *CD4060BM Datasheet*, Texas Instruments, 2013. Available from: <http://www.ti.com/lit/ds/symlink/cd4060bm.pdf>.
- [44] García del Castillo, C., *Diseño e implementación de las antenas y los sistemas de transmisión y recepción de un CubeSat*. Final project. Polytechnic University of Catalonia (UPC), 2012.

## A Link budget



## B Technical drawing of the antenna holder and the end plate



## C Radiation pattern

